2 Two-Body Interaction

Learning Objectives

- Highlight "short-ranged," "dilute," and "low energy" as three main features of interactions between ultracold atoms.
- Introduce the important concept of the phase shift.
- Introduce the *s*-wave scattering length as a universal parameter describing the low-energy interaction between ultracold atoms.
- Discuss the relation between divergent scattering length, low-energy bound state, and jump of phase shift.
- Discuss the relation between the scattering length and the scattering amplitude.
- Discuss under what conditions a positive scattering length describes repulsive interaction.
- Discuss the conditions when an algebraically decayed potential can be treated as a finite range one.
- Introduce two types of zero-range single-channel potentials to capture the universal low-energy *s*-wave interaction between ultracold atoms.
- Introduce the concepts of renormalization condition and renormalizable theory.
- Discuss how the spin rotational symmetry imposes constraints on interaction forms for both alkali-metal and alkaline-earth-metal atoms.
- Introduce Feshbach resonance as an important tool to tune scattering length.
- Compare the two-channel Feshbach resonance with the single-channel shape resonance, and compare wide and narrow resonances.
- Introduce a zero-range two-channel model.
- Introduce the confinement-induced resonance to tune interaction strength by an external potential.
- Summarize three key conditions for a Feshbach resonance, and unify the optical Feshbach resonance, the orbital Feshbach resonance, and the confinement induce resonance all in terms of these three conditions.
- Introduce the Efimov effect as an important three-body effect at the vicinity of the two-body scattering resonance.
- Highlight the symmetry aspect of the Efimov effect.
- Discuss various connections between few-body and many-body physics.
- Illustrate that few-body calculation can be used to determine properties of many-body systems by using high-temperature expansion as an example.

https://doi.org/10.1017/9781108595216.003 Published online by Cambridge University Press

2.1 Scattering Length

Interactions between particles play the most important role in quantum many-body physics. One of the major common goals of both ultracold atomic physics and condensed matter physics is to understand interaction effects in quantum many-body systems. Ultracold atomic physics studies dilute gases of neutral atoms, and condensed matter physics mainly focuses on electronic gases in solid. Many fundamental differences between the many-body phenomena in these two systems can be traced back to the different interaction forms between particles in these two systems. The interaction between electrons are the Coulomb repulsion, and the interatomic potential contains an attractive Van der Waals potential and a strong repulsion at very short distance. This interaction between ultracold atoms possesses the following three key features that are important for our subsequent discussions.

- Short Ranged: The Van der Waals interaction $V(\mathbf{r})$ is short ranged, and to a certain extent, we can approximate $V(\mathbf{r}) \simeq 0$ when $r > r_0$, where r_0 is the range of the potential.
- Dilute: The ultracold atomic gas is very dilute, and the typical distance d between two atoms is much larger than r_0.
- Low Energy: The temperature of ultracold atomic gas is very low; that is to say, the incoming energy $E = \hbar^2 k^2/(m)$ of the scattering state is very low compared with the short-range potential energy, that is, $kr_0 \ll 1$, or equivalently, $\hbar^2 k^2/(m) \ll \hbar^2/(mr_0^2)$.

With the first two points, it seems that for most of the time, any two atoms are far separated at a distance where the interaction potential is zero. Thus, classically atoms do not experience any forces mutually and the gas looks like a noninteracting one. However, as we will show in this chapter, in the quantum regime, this system is not only an interacting one but also sometimes can become a strongly interacting one.

The Phase Shift. Let us consider a two-body Schrödinger equation in the relative coordinate

$$\left[-\frac{\hbar^2}{2\bar{m}}\nabla^2 + V(\mathbf{r})\right]\Psi = E\Psi, \tag{2.1}$$

where $\mathbf{r}$ stands for the relative coordinate between two atoms, $\bar{m}$ is the reduced mass of two particles, and $\bar{m} = m/2$ for particles with equal mass m. Here we focus on the situation that $V(\mathbf{r})$ is spherical symmetric,[1] and we can expand the wave function in terms of different angular momentum partial waves as

$$\Psi(\mathbf{r}) = \sum_{l=0}^{+\infty} \frac{\chi_{kl}(r)}{kr}\mathcal{P}_l(\cos\theta), \tag{2.2}$$

and different partial waves are decoupled. It is easy to show that

$$\frac{d^2\chi_{kl}}{dr^2} - \frac{l(l+1)}{r^2}\chi_{kl} + \frac{2\bar{m}}{\hbar^2}(E - V(r))\chi_{kl} = 0. \tag{2.3}$$

[1] For atoms like dysprosium and erbium with partially filled f-shells, as we discussed in Section 1.1, the Van der Waals interaction is anisotropic in the presence of an external magnetic field, and there also presents an anisotropic dipolar interaction. Here we do not discuss this situation.

https://doi.org/10.1017/9781108595216.003 Published online by Cambridge University Press

We first consider the s-wave scattering channel with $l = 0$. Because of the short-ranged nature of the potential, for $r > r_0$, $V(r) = 0$, and in this regime a general solution to Eq. 2.3 is given by

$$\chi_k = A \sin(kr + \delta_k), \tag{2.4}$$

where δ_k is called the *phase shift*. The phase shift is the most important quantity for low-energy scattering in a dilute quantum gas. Because of the dilute nature of the ultracold atomic gas stated above, atoms have a negligible chance to come close enough to explore the details of the interaction potential, and therefore we are only concerned about the wave function in the regime $r \gg r_0$. It is clear that all the interaction effects are contained in the phase shift δ_k.

However, the phase shift is determined by the behavior of the wave function at short distance. To determine δ_k, we need the information in the regime with $r < r_0$. We shall match the boundary condition at $r = r_0$ to give

$$\left.\frac{\chi'(r > r_0)}{\chi(r > r_0)}\right|_{r=r_0} = \frac{k\cos(kr_0 + \delta_k)}{\sin(kr_0 + \delta_k)} \simeq \frac{k}{\tan\delta_k} = \left.\frac{\chi'(r < r_0)}{\chi(r < r_0)}\right|_{r=r_0}. \tag{2.5}$$

Here, for the second approximate equality, we have used the low-energy property to approximate $kr_0 \approx 0$. Now, the question is, to determine the phase shift, do we need to know the full information of the wave function $\chi(r < r_0)$ inside $r < r_0$? Let us consider the situation that when $r < r_0$, the interaction potential changes very rapidly, and in this regime, the incoming energy E can be ignored compared with the strength of $V(\mathbf{r})$. Thus, it is reasonable to assume that the energy E dependence of $\chi(r < r_0)$ is insignificant for the low-energy states. Therefore, to the leading order, we can take $\chi'(r < r_0)/\chi(r < r_0)|_{r=r_0}$ simply as a constant denoted by $-1/a_s$, where a_s is called the *s-wave scattering length*. Thus we have

$$\frac{k}{\tan\delta_k} = -\frac{1}{a_s}. \tag{2.6}$$

With Eq. 2.6 the relation between δ_k and k is shown in Figure 2.1. It shows that for small k, δ_k linearly depends on momentum as $-ka_s$, and for large k (but still much smaller compared with $1/r_0$), δ_k saturates to $\pm\pi/2$. We should also note that for deriving Eq. 2.6, we only use the three conditions discussed at the beginning, and Eq. 2.6 is therefore valid for any value of a_s, including $a_s = \pm\infty$. As shown in Figure 2.1, when a_s becomes larger, the linear regime of δ_k becomes smaller. When $a_s = \pm\infty$, δ_k becomes $\mp\pi/2$ for any nonzero k.

We can further treat E as a perturbation for the Schrödinger equation in the regime $r < r_0$ and improve this expansion systematically. By expanding $k/\tan\delta_k$ to the next order in k^2, we obtain

$$\frac{k}{\tan\delta_k} = -\frac{1}{a_s} + \frac{1}{2}r_{\text{eff}}k^2 + \ldots, \tag{2.7}$$

where the coefficient defines an effective range r_{eff}. In most cases, the contribution from the r_{eff} term is negligible at low energy, and a_s is the most important parameter for describing low-energy two-body interactions. However, there are exceptions. For example, when a_s

https://doi.org/10.1017/9781108595216.003 Published online by Cambridge University Press

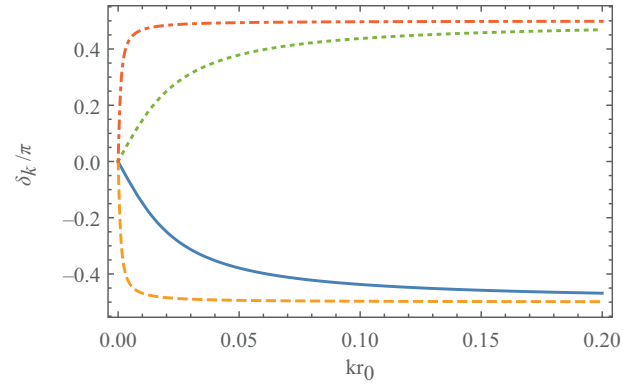

Figure 2.1 The s-wave phase shift. The phase shift δ_k/π as a function of kr_0 for different a_s/r_0; $a_s/r_0 = 50$ for the solid line, $a_s/r_0 = 10^3$ for the dashed line, $a_s/r_0 = -50$ for the dotted line, and $a_s/r_0 = -10^3$ for the dash-dotted line. A color version of this figure can be found in the resources tab for this book at cambridge.org/zhai.

approaches zero, the expansion equation 2.7 is not very appropriate because δ_k cannot be always zero for all k. In the limit $a_s \to 0$, it is better to expand [19]

$$-\frac{\tan\delta_k}{k} = \frac{1}{\frac{1}{a_s} - \frac{1}{2}r_{\text{eff}}k^2} \approx a_s + \frac{1}{2}r_{\text{eff}}a_s^2k^2 + \ldots. \tag{2.8}$$

In fact, in the limit $a_s \to 0$, r_{eff} diverges such that $r_{\text{eff}}a_s^2$ remains finite, and $v = -r_{\text{eff}}a_s^2$ is called the *scattering volume*. That is to say, when a_s is finite, $\tan\delta_k$ linearly depends on k, and when a_s vanishes, the linear term vanishes and $\tan\delta_k$ depends on $\sim k^3$.

Considering two different short-range potentials $V_1(\mathbf{r})$ and $V_2(\mathbf{r})$, say, for two interaction potentials of two different atoms, the short-range wave functions $\chi_1(r)$ and $\chi_2(r)$ are also very different in the regime $r < r_0$. But as long as they give the same value of χ'/χ at $r = r_0$ and therefore the same phase shift, the low-energy physics of the two systems are identical, despite the very different behaviors of the short-range potentials. If we further focus on the situation that the effective range effect is negligible, then these two potentials share the same a_s, and this a_s is the only parameter that is needed for describing the low energy of two different microscopic potentials. This is so-called *universality*, which states that different systems with quite different microscopic details can be described universally by a few parameters.

The s-wave scattering length also possesses a clear geometric meaning. In the zero-energy limit, the s-wave wave function at $r > r_0$ can be expanded as

$$\begin{aligned}\chi(r) &\propto \sin(kr + \delta_k) \approx \sin\delta_k + \cos\delta_k(kr)\\ &\propto 1 + \frac{k}{\tan\delta_k}r = 1 - \frac{r}{a_s}.\end{aligned} \tag{2.9}$$

It is clear that $\chi(r = a_s) = 0$; that is to say, a_s is the location of the node of the zero-energy radial wave function.

Let us consider a toy model with a finite range attractive square well potential $V(r) = -V_0$ ($V_0 > 0$) for $0 < r < r_0$, and $V(r) = 0$ for $r > r_0$, and we also consider a hard core

https://doi.org/10.1017/9781108595216.003 Published online by Cambridge University Press

boundary condition at $r = 0$. This simple toy model mimics the real interatomic potential. In this model, the zero-energy wave function for $0 < r < r_0$ is given by

$$\chi(r) = \sin\left(\sqrt{\frac{2V_0\bar{m}}{\hbar^2}}r\right). \tag{2.10}$$

It satisfies the hard core boundary condition at $r = 0$, and its slope at $r = r_0$ determines the wave function at the outside, whose node determines a_s. With this picture, it is easy to show how a_s changes as the depth V_0 of the attractive well increases. When the attractive well is shallow and $\sqrt{2V_0\bar{m}/\hbar^2}r_0 < \pi/2$, the situation is shown in the left of Figure 2.2(a), where the node of the wave function appears at a negative value, giving rise to a negative a_s. As V_0 increases, when $\sqrt{2V_0\bar{m}/\hbar^2}r_0$ approaches $\pi/2$, the slope for the zero-energy wave function approaches zero. As a result, a_s first approaches $-\infty$, and then jumps from $-\infty$ to $+\infty$, as shown in the middle of Figure 2.2(a). At this jump, the phase shift also jumps from $\pi/2$ to $-\pi/2$. Then, when V_0 further increases, the slope becomes negative and the node comes to a positive value, as shown in the right of Figure 2.2(a). As V_0 further increases, a_s decreases from $+\infty$ to finite positive value. This simple example shows that a_s can take any value from $-\infty$ to $+\infty$, as we shown in Figure 2.2(b).

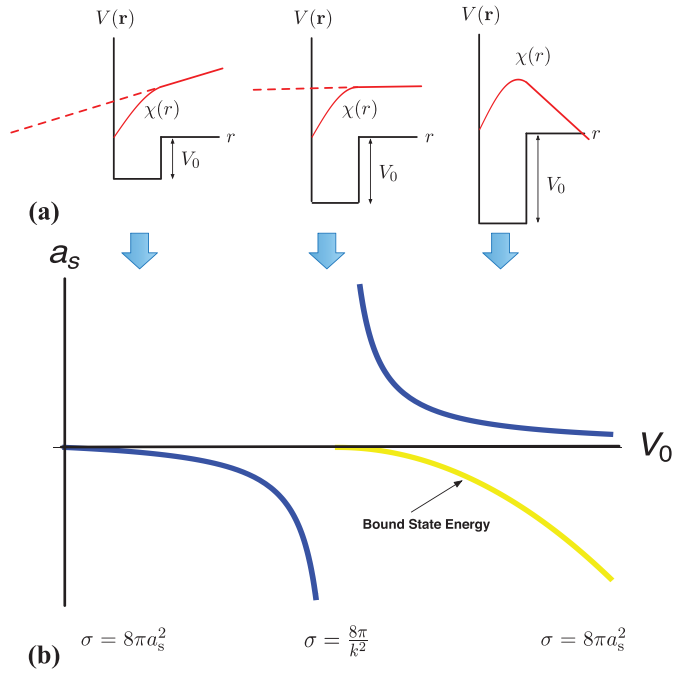

Figure 2.2 Geometric meaning of the scattering length. (a) The geometric meaning of the s-wave scattering length illustrated by a square well model. (b) The s-wave scattering length as a function of the depth of the attractive well. The low-energy bound state energy is also plotted. Different behaviors of the scattering amplitudes are marked in different regimes. A color version of this figure can be found in the resources tab for this book at cambridge.org/zhai.

https://doi.org/10.1017/9781108595216.003 Published online by Cambridge University Press

In this simple toy model, it can also be shown that

$$-\frac{1}{a_s}=\left.\frac{\chi'(r<r_0)}{\chi(r<r_0)}\right|_{r=r_0}=\frac{\sqrt{\frac{2V_0\bar{m}}{\hbar^2}}}{\tan\left(\sqrt{\frac{2V_0\bar{m}}{\hbar^2}}r_0\right)}. \tag{2.11}$$

It is clear that a_s will repeatedly change from ∞ to $+\infty$ as V_0 increases. That is to say, there will be a series of different values of V_0 that give the same value of a_s. With our discussion of universality above, this means that the low-energy physics is the same for these different values of V_0.

Finally, it is worth mentioning that the discussion of the phase shift can be generalized to other higher partial waves. One can show that for the lth partial wave, the corresponding phase shift $\delta_k \propto k^{2l+1}$. Therefore, for low-energy collision, the phase shifts for the higher partial waves are suppressed compared with the s-wave case. That means that at the lowest energy, the interaction effect is dominated by the s-wave channel, as long as the s-wave channel is not forbidden.

The Shallow Bound State. Above we have considered low-energy scattering states with $E > 0$, and now we turn to consider a bound state with negative energy $E < 0$. The difference between a scattering state and a bound state lies on the asymptotic behavior at large r. For scattering states, their wave functions keep oscillating with a fixed momentum at large r. The energy spectrum of scattering states is a continuum, and the short-range boundary condition determines the phase shift. But for bound states, their wave functions decay exponentially at large r, and the energy spectrum of bound states is discrete, which is determined by the short-range boundary condition. Explicitly, in the regime $r > r_0$, the radial wave function is given by

$$\chi = Ae^{-r\sqrt{2\bar{m}|E|/\hbar^2}}. \tag{2.12}$$

Similarly to the discussion of the low-energy scattering state, here we are concerned with the absolute value of the binding energy being much weaker than the strength of the potential, such that the wave function at the short distance $r < r_0$ is also insensitive to the bound state energy. Therefore, we can match the same boundary condition at $r = r_0$ for this bound state wave function and reach

$$\left.\frac{\chi'}{\chi}\right|_{r=r_0}=-\sqrt{\frac{2\bar{m}|E|}{\hbar^2}}=-\frac{1}{a_s}. \tag{2.13}$$

Obviously, if $a_s < 0$, there is no solution for Eq. 2.13, which means that there is no shallow bound state for negative a_s. But for $a_s > 0$, we have a bound state solution with

$$E_b=-\frac{\hbar^2}{2\bar{m}a_s^2}, \tag{2.14}$$

which is shown in Figure 2.2(b).

Nevertheless, we should be very careful about the statement of no bound state with negative a_s. In fact, as shown in Figure 2.2, the first bound state appears at $\sqrt{2V_0\bar{m}/\hbar^2}r_0 = \pi/2$, and it will not disappear when V_0 further increases. However, there are regimes with

https://doi.org/10.1017/9781108595216.003 Published online by Cambridge University Press

larger V_0 where a_s is negative. That is to say, for these negative a_s, there actually exist bound states. To reconcile this fact with Eq. 2.13 above, we should note that Eq. 2.13 only applies to the low-energy bound state because of the assumption that boundary conditions are insensitive to energy. The absence of a solution for Eq. 2.13 only rules out the existence of the low-energy bound state but does not exclude the existence of deep bound states. In fact, it is easy to see that the bound state that emerged at $\sqrt{2V_0\bar{m}/\hbar^2}r_0 = \pi/2$ becomes a sufficient deep bound state when a_s becomes negative again. Moreover, even for positive a_s, Eq. 2.14 works only when $a_s/r_0 \gg 1$. The binding energy will deviate from this universal expression, and the short-range details will matter when the bound state is sufficiently deep.

Features of a Scattering Resonance. From above discussions, we can also find that the following three properties occur simultaneously, which we call an *s-wave scattering resonance*:

1. The s-wave scattering length jumps from $-\infty$ to $+\infty$.
2. The phase shift jumps by π.
3. A bound state appears at the threshold.

This connection between the jump of the phase shift and the existence of a zero-energy bound state is also related to Levinson's theorem in quantum mechanics.

Now we have introduced the scattering length a_s as a central concept for the s-wave scattering. Below we will address two important questions regarding how to interpret the physical meaning of a_s.

In What Sense Does a Larger $|a_s|$ Mean a Stronger Interaction? We have considered the two-body problem from the perspective of the eigenstate of the Schrödinger equation. Here we introduce another viewpoint. Considering an incoming wave e^{ikz} along the $\hat{z}$ direction that is scattered to an outgoing wave along the radial direction, the total wave function at large distance can be written as

$$\Psi = e^{ikz} + f(\theta)\frac{e^{ikr}}{r}, \tag{2.15}$$

where $f(\theta)$ is called the *scattering amplitude*. To determine $f(\theta)$, we need to first rewrite Eq. 2.15 as

$$\Psi = \frac{1}{2ikr}\left[\sum_{l=0}^{+\infty}(2l+1)\mathcal{P}_l(\cos\theta)(e^{ikr-l\pi/2} - e^{-i(kr-\pi l/2)})\right] + f(\theta)\frac{e^{ikr}}{r}. \tag{2.16}$$

Because these two viewpoints should give the same results, by comparing this equation with Eq. 2.2 and Eq. 2.4, and focusing on the $l = 0$ channel, we can obtain the s-wave scattering amplitude as

$$f_s(\theta) = \frac{e^{2i\delta} - 1}{2ik} = -\frac{1}{ik - k/\tan\delta} = -\frac{1}{1/a_s + ik}, \tag{2.17}$$

which is independent of θ. For identical bosons, the scattering cross section σ is given by $8\pi|f_s|^2$. If $|ka_s| \ll 1$, we have $f(\theta) \sim -a_s$, and the scattering cross section is $\sigma = 8\pi a_s^2$. Thus, the larger $|a_s|$ is, the larger is the scattering cross section. In this sense, one can say

https://doi.org/10.1017/9781108595216.003 Published online by Cambridge University Press

that the absolute value of a_s represents the strength of the interaction. But this argument cannot be generalized to very large or even infinite a_s, because if $|ka_s| \gg 1$, $f(\theta)$ should be approximated as $-1/(ik)$, and then the scattering cross section becomes $8\pi/k^2$. It is interesting to note that in this regime, the scattering cross section strongly depends on momentum of particles under collision and does not depend on any other parameters. This is the so-called unitary regime. As already indicated in this formula of the scattering cross section, the interaction energy of a many-body system at the unitary regime only depends on density and temperature. These behaviors will be discussed in Chapters 5 and 6 in detail.

In What Sense Does $a_s > 0$ Mean Repulsive Interaction? When we talk about a pure short-range repulsive interaction, usually what we naturally have in mind is a hard core potential with size R_0. That is to say, $V(r) = +\infty$ for $r \leqslant R_0$ and $V(r) = 0$ for $r > R_0$, which forces the wave function to vanish at $r = R_0$. This leads to $\delta_k = -kR_0$. The interatomic interaction we considered here has an attractive well, and the microscopic potential form is very different from the hard core potential. However, the low-energy expansion of the phase shift given by Eq. 2.6 can agree with $\delta_k = -kR_0$, at least for a large range of small k, if a_s is positive and $a_s = R_0$. Therefore, as far as the low-energy phase shift of the scattering states is concerned, a positive a_s is equivalent to a hard core repulsive interaction. In other words, as we discussed at the beginning of this section, atoms in a dilute gas can only experience the phase shift δ_k, so they cannot distinguish the actual interatomic potential from a hard core potential for sufficiently low-energy atoms.

However, we shall emphasize that this equivalence is only valid for low-energy scattering states and small a_s such that $ka_s \ll 1$. There are several reasons. First, at large momentum, when ka_s is large, the phase shift given by Eq. 2.6 always saturates to $-\pi/2$, but the phase shift of a hard core potential keeps increasing linearly. Second, in order for the hard core model to be valid in a gas system, the hard core radius R_0 should be taken to be much smaller than the interparticle spacing, typically $1/k$. That also requires $a_s \sim R_0 \ll 1/k$. Third, as discussed above, for positive a_s, there is a low-energy bound state, and such a bound state is also absent in the hard core potential. Nevertheless, only when $ka_s \ll 1$, the absolute value of the binding energy $\hbar^2/(2\bar{m}a_s^2)$ is much larger than typical kinetic energy $\hbar^2k^2/(2\bar{m})$, and this bound state is well beyond the low-energy regime. In summary, a positive a_s can be regarded as representing a repulsive interaction only when

1. $ka_s \ll 1$ and only the low-energy scattering states are considered.
2. the bound state is sufficiently deep that can be safely ignored for low-energy scattering.

How Short Range Is Short Ranged? So far, we have considered a finite range potential where the interaction is taken strictly as zero above a range r_0. But the actual Van der Waals potential is algebraically decaying one at large distance. Now we shall come back to briefly revisit how good this approximation is to replace an algebraically decaying potential as a strictly finite-range one.

Let us again first recall how we solve the finite-range potential. In the $r > r_0$ regime, the potential term vanishes and the Hamiltonian only contains the kinetic energy term. For a three-dimensional kinetic operator, there are two independent solutions for the s-wave

https://doi.org/10.1017/9781108595216.003 Published online by Cambridge University Press

Box 2.1 Meaning of Positive Scattering Lengths in This Book

Since the main part of this book discusses interaction effects in ultracold atomic gases, here we shall make an important statement on modeling the interaction potential in different parts of this book. In Parts II and IV of this book, we always consider the situation that the scattering length is small compared with the interatomic distance. Hence, when we talk about positive a_s, by default, we consider that these two conditions are satisfied, and the interaction is taken as repulsive. In Part III of this book, we will consider the situation that a_s can go across infinity. In this case, these two conditions are not satisfied, and in particular, the role of the shallow bound state is very crucial. In this part, a positive a_s does not mean the interaction is repulsive.

channel, which can be taken as $\sin(kr)/(kr)$ and $\cos(kr)/(kr)$. The general wave function at large distance is a superposition of these two solutions, and the mixing angle of the superposition gives the phase shift, which should be determined by the short-range physics.

This strategy can be generalized straightforwardly to an algebraically decaying potential. The only difference is that one needs to find out the corresponding solutions for a $1/r^{\alpha}$ potential. It turns out that, for the s-wave case, one can also write down two independent solutions whose asymptotic behavior also approaches $\sin(kr)/(kr)$ and $\cos(kr)/(kr)$, respectively. Hence, the general wave function is a superposition of these two solutions, and the mixing angle of the superposition determines the phase shift in this case. In this case, the phase shift is also determined by the short-range physics. The similar treatment can be generalized to higher partial wave cases. In this way, one can show that for the lth partial wave, $\tan\delta_k \propto k^{2l+1}$ if $2l+1 \leq \alpha-2$ and $\tan\delta_k \propto k^{\alpha-2}$ if $2l+1 \geq \alpha-2$ [34]. Therefore, as far as the low-energy physics is concerned, if an algebraically decaying potential is considered to be equivalent to a finite-range one, at least the leading-order contribution to the low-energy phase shift has to be the same for these two potentials, which means $\alpha-2$ has to be larger than $2l+1$. Thus, for the s-wave channel, α should be greater than 3. For the realistic Van der Waals potential, $\alpha = 6$, and this means that for $l = 0, 1$ channels, it can be treated by the strictly finite-range approximation, and for $l \geq 2$, the algebraically decaying tail needs to be considered more seriously.

2.2 Zero-Range Models

We have discussed the low-energy physics for a two-body problem using a finite-range potential and shown that for most circumstances, the s-wave scattering length a_s is the only parameter that is required for describing the low-energy interaction in a dilute quantum gas. Here we would like to develop an effective model to describe the interaction effects in many-body systems, and we would like to require the following two features in our effective model:

https://doi.org/10.1017/9781108595216.003 Published online by Cambridge University Press

- Inspired by the two-body discussion, we would like to use the s-wave scattering length a_s as the only parameter in our effective model and disregard the microscopic details of the interatomic potential.
- For the convenience of later studies of many-body theories, it will be useful that this effective model is a zero-range one, that is to say, two atoms interact only when they are exactly in the same spatial location. In Section 2.1, we always keep the interaction range r_0 finite, and in this section, we should be taking r_0 to zero.

Here, by *effective*, we mean that the low-energy scattering properties, including phase shift for the low-energy scattering state and the shallow bound state energy, can be well reproduced by this effective model. Below we present two different effective models, and both can achieve this goal.

Pseudopotential. The simplest form of a zero-range model is a delta-function potential $V(\mathbf{r}) \propto \delta(\mathbf{r})$. Obviously, for $r \neq 0$, $V(\mathbf{r}) = 0$ and $\chi(r) = \sin(kr + \delta_k)$ always satisfy the Schrödinger equation. The question is whether the Schrödinger equation can still be satisfied as $r \to 0$. However, as shown above, for zero energy, $\chi(r)$ behaves as $1 - r/a_s$ and therefore $\Psi(r)$ behaves as $1/r - 1/a_s$, which diverges as $1/r$ at the short distance. Therefore, a simple delta-function potential gives a divergent energy. We note that this $1/r$ divergence is not physical, because in the finite-range model discussed above, the free wave function terminates at r_0 and the even short-range wave function is determined by the microscopic potential. In other words, this $1/r$ divergence is an artifact arising from taking r_0 to zero. So a properly defined interaction potential should be able to eliminate this $1/r$ divergency at $r \to 0$ before taking the δ-function interaction.

Let us denote such a potential as $V(\mathbf{r}) = \delta(\mathbf{r})\hat{\mathcal{O}}(r)$, and $V(\mathbf{r})$ should satisfy the Schrödinger equation as

$$\left[-\frac{\hbar^2}{2\bar{m}}\nabla^2 + V(\mathbf{r})\right]\Psi = E\Psi, \tag{2.18}$$

where $\Psi(r) = \sin(kr + \delta_k)/(kr)$. To focus on the $r \to 0$ limit, let us again consider the expansion of the wave function $\Psi(r)$ around $r = 0$ as

$$\Psi(r) = \frac{1}{r} - \frac{1}{a_s} + o(kr). \tag{2.19}$$

It is straightforward to show that

$$[\partial_r \cdot r]\Psi(r) = -\frac{1}{a_s} + o(kr), \tag{2.20}$$

which eliminates the short-range $1/r$ divergence. Hence, when $\hat{O}(r)$ takes the form [77]

$$\hat{O}(r) = \frac{2\pi\hbar^2 a_s}{\bar{m}}\partial_r \cdot r, \tag{2.21}$$

we have

$$V(\mathbf{r})\Psi(r) = -\frac{2\pi\hbar^2}{\bar{m}}\delta(\mathbf{r}). \tag{2.22}$$

https://doi.org/10.1017/9781108595216.003 Published online by Cambridge University Press

And because in three dimensions,

$$-\frac{\hbar^2}{2\bar{m}}\nabla^2\Psi(r) = \frac{2\pi\hbar^2}{\bar{m}}\delta(\mathbf{r}), \tag{2.23}$$

the Schrödinger equation is satisfied. This interaction potential is known as Fermi's pseudo-potential [77]. Furthermore, one can show that the energy of the low-energy bound state can also be reproduced.

Renomalizable Contact Potential. A pseudo-potential model can nicely reproduce the low-energy physics. However, it has a shortcoming that the operator is not Hermitian. Thus, it is not very convenient to use the pseudo-potential in many circumstances, in particular, when a second-quantized form of a many-body Hamiltonian is needed. For studying many-body physics, it is still convenient to use a delta-function contact potential as $V(\mathbf{r}) = g\delta(\mathbf{r})$. Though we have already known that it will cause a divergent problem at short distance, nevertheless, let us proceed further and see how serious the problem is and whether there are ways to fix the problem.

Here we consider spin-1/2 fermions with this delta-function interaction potential as an example. With a delta-function interaction potential, the second-quantized Hamiltonian for spin-1/2 fermions can be written as

$$\hat{\mathcal{H}} = \int d^3\mathbf{r}\left(\sum_\sigma \hat{\Psi}^\dagger_\sigma(\mathbf{r})\left(-\frac{\hbar^2}{2m}\nabla^2\right)\hat{\Psi}_\sigma(\mathbf{r}) + g\hat{\Psi}^\dagger_\uparrow(\mathbf{r})\hat{\Psi}^\dagger_\downarrow(\mathbf{r})\hat{\Psi}_\downarrow(\mathbf{r})\hat{\Psi}_\uparrow(\mathbf{r})\right), \tag{2.24}$$

where $\hat{\Psi}^\dagger_\sigma(\mathbf{r})$ and $\hat{\Psi}_\sigma(\mathbf{r})$ ($\sigma = \uparrow, \downarrow$) are creation and annihilation operators for fermions at position $\mathbf{r}$. In the momentum space, this Hamiltonian is given by

$$\hat{\mathcal{H}} = \sum_{\mathbf{k}\sigma}\frac{\hbar^2\mathbf{k}^2}{2m}\Psi^\dagger_{\mathbf{k}\sigma}\Psi_{\mathbf{k}\sigma} + \frac{g}{V}\sum_{\mathbf{k},\mathbf{k_1},\mathbf{k_2}}\hat{\Psi}^\dagger_{\frac{\mathbf{k}}{2}+\mathbf{k}_{\mathbf{1},\uparrow}}\hat{\Psi}^\dagger_{\frac{\mathbf{k}}{2}-\mathbf{k}_{\mathbf{1},\downarrow}}\hat{\Psi}_{\frac{\mathbf{k}}{2}-\mathbf{k}_{\mathbf{2},\downarrow}}\hat{\Psi}_{\frac{\mathbf{k}}{2}+\mathbf{k}_{\mathbf{2},\uparrow}}, \tag{2.25}$$

where V is the volume of the system. Here the second term represents scattering between atoms, with the center-of-mass momentum $\mathbf{k}$ conserved and the relative momenta changing from $\mathbf{k_2}$ to $\mathbf{k_1}$.

We first compute a two-body scattering T-matrix with Hamiltonian equation 2.25. We consider an on-shell scattering process with both incoming and outgoing states having the same energy E and the center-of-mass momentum equaling zero. Since the interaction vertex g is now a constant independent of momentum, the leading order diagram is a direct scattering from the incoming state to the outgoing state, whose contribution is g, as shown in Figure 2.3(a). The next-order diagram involves intermediate states, and the relative momentum $\mathbf{p}$ of the intermediate state can be taken at any momentum. Its contribution can be computed by the second-order processes as

$$\frac{1}{V}\sum_{\mathbf{p}} g\frac{1}{E - \frac{\hbar^2\mathbf{p}^2}{m} + i0^+}g, \tag{2.26}$$

where $i0^+$ is a mathematical technicality necessary for the calculation of the integrals and is also a consequence of causality. Furthermore, one can systematically consider all the

https://doi.org/10.1017/9781108595216.003 Published online by Cambridge University Press

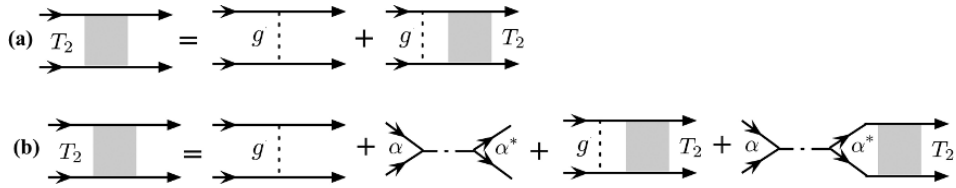

Figure 2.3 T-matrix for two-body scattering. Ladder diagrams for two-body T-matrix (a) of the renormalizable contact potential model Eq. 2.24 and (b) for the two-channel model Eq. 2.66. The two-channel model will be discussed in Section 2.4.

higher order contributions by including more intermediate states, as illustrated by the so-called ladder diagram shown in Figure 2.3(a). It turns out that for two-body problems, unlike the many-body situation to be discussed in later chapters, the summation of the ladder diagram is an exact solution. The summation of the ladder diagram leads to the so-called *Schwinger–Dyson equation* given by

$$\begin{aligned} T_2(E) &= g + \frac{1}{V}\sum_{\mathbf{p}} g \frac{1}{E - \frac{\hbar^2\mathbf{p}^2}{m} + i0^+} g + \dots \\ &= g + \frac{g}{V}\sum_{\mathbf{p}} \frac{1}{E - \frac{\hbar^2\,\mathbf{p}^2}{m} + i0^+} T_2(E), \end{aligned} \tag{2.27}$$

and thus

$$T_2(E) = \frac{g}{1 - \frac{g}{V}\sum_{\mathbf{p}} \frac{1}{E - \frac{\hbar^2\mathbf{p}^2}{m} + i0^+}}. \tag{2.28}$$

Here it is important to notice that the summation over momentum in Eq. 2.28 behaves as $\int d^3\mathbf{p}(1/p^2)$ at large momentum and diverges at large momentum in three dimensions. This divergence comes from the upper limit of the energy integration and is called the *ultraviolet divergence*. As we discussed in Box 2.2, such an ultraviolet divergence means the short-range physics is not treated properly. Here, it means nothing but that the short-range $1/r$ behavior of the free wave function should not be taken to the $r \to 0$ limit, and the δ-function contact potential is not appropriate.

This divergence can also be viewed from the Hamiltonian in momentum space equation 2.25, where the scattering vertex is taken as independent of the momentum transfer, because the Fourier transformation of a δ-function potential is a constant. However, this is unphysical because in any physical model with finite range r_0, this scattering vertex always decays toward zero when the transferred momentum is much larger than $\hbar/r_0$. By taking this momentum dependence of the scattering vertex into account, the large momentum divergence in the summation of Eq. 2.28 can be avoided. Nevertheless, the momentum dependence of the scattering vertex at large momentum comes from the short-range structure of the microscopic potential, which is the nonuniversal physics that we do not want to include.

Hence, we encounter a dilemma. On one hand, we understand that the zero-range δ-function potential, or equivalently saying, a momentum-independent scattering vertex at large momentum, is unphysical, which causes ultraviolet divergence. On the other hand,

https://doi.org/10.1017/9781108595216.003 Published online by Cambridge University Press

Box 2.2 Two Kinds of Divergences

Quite often, we will encounter the situation that the integration over energy, or equivalently, the integration over momentum space, diverges. There are two different kinds of divergence. One is called the ultraviolet divergence, and the other is called the infrared divergence. The ultraviolet divergence is due to the upper limit of the energy integration taking to infinity, and the infrared divergence is due to the lower limit of the energy integration taking to zero. However, the physical quantity should always be finite. Thus, both divergences mean that something unphysical is mistaken. The ultraviolet divergence usually means that the high-energy physics, or equivalently, the short-range physics, is not treated properly. Here the delta-function potential is such an example. The infrared divergence usually means the low-energy, or equivalently, the large-scale structure, is mistaken. We will discuss an example of the infrared divergence in Section 3.4.

the details of the short-range potential, or the momentum dependence of the scattering vertex at large momentum, is nonuniversal, which we do not want to explicitly include. To overcome this problem, we will implement the idea of *renormalization*. We will still use the delta-function potential, but we will not treat interaction parameter g as a physical parameter. And we should find a way to properly renormalize the interaction parameter g and to relate it to the physical parameter a_s. Hence, let us rewrite

$$\begin{aligned} T_2(E) &= \frac{g}{1-\frac{g}{V}\sum_{\mathbf{p}}\frac{1}{E-\hbar^2\mathbf{p}^2/(m)+i0^+}} \\ &= \frac{1}{\frac{1}{g}+\frac{1}{V}\sum_{\mathbf{p}}\frac{1}{\hbar^2\,\mathbf{p}^2/m}-\frac{1}{V}\sum_{\mathbf{p}}\left(\frac{1}{E-\frac{\hbar^2\,\mathbf{p}^2}{m}+i0^+}+\frac{1}{\hbar^2\mathbf{p}^2/m}\right)} \\ &= \frac{1}{\frac{1}{g}+\frac{1}{V}\sum_{\mathbf{p}}\frac{1}{\hbar^2\,\mathbf{p}^2/m}+\frac{ikm}{4\pi\hbar^2}}, \end{aligned} \tag{2.29}$$

where $k=\sqrt{mE/\hbar^2}$. This two-body T-matrix should be related to the s-wave scattering amplitude of Eq. 2.17 determined by the two-body calculation above; therefore, we have

$$T_2(E)=\frac{4\pi\hbar^2}{m}\frac{1}{\frac{1}{a_s}+ik}=\frac{1}{\frac{1}{g}+\frac{1}{V}\sum_{\mathbf{p}}\frac{1}{\hbar^2\mathbf{p}^2/m}+\frac{ikm}{4\pi\hbar^2}}. \tag{2.30}$$

Hence, we reach the important renormalization identity that relates g to physical quantity a_s, that is,

$$\frac{m}{4\pi\hbar^2 a_s}=\frac{1}{g}+\frac{1}{V}\sum_{\mathbf{p}}\frac{1}{\hbar^2\mathbf{p}^2/m}. \tag{2.31}$$

To conclude, we will use Eq. 2.24 or Eq. 2.25 as our model for a many-body system. But one will often encounter an ultraviolet divergence problem when using this model. When the ultraviolet divergence is encountered, we should use Eq. 2.31 to replace g by

https://doi.org/10.1017/9781108595216.003 Published online by Cambridge University Press

the physical parameter a_s, and at the same time this replacement eliminates the divergency. This is an important result that will be repeatedly used in later chapters.

However, there is one important question. Here we obtain the renormalization condition by matching the two-body scattering amplitude. How can we be sure that this renormalization condition can work for a system with more than two particles? In general, the answer is that it may or may not work. If this works, the theory is called *renormalizable*. If this does not work, it means some extra high-energy scales emerge in few- or many-body systems, and these energy scales matter. In fact, as we will see in Chapter 5 and Chapter 6, theory for spin-$1/2$ fermion is renormalizable. But for spinless bosons, the renormalization condition actually does not work. This can be seen from Section 2.6, where we will discuss the three-body problem for bosons. We will see that an extra high-energy cutoff scale is required for the energy spectrum being bounded from below.

2.3 Spin-Dependent Interaction

In the discussion above, we do not explicitly include the role of the spin degree of freedom of the atoms under collision. From Section 1.1 we already know that atoms can have quite rich spin structures, and we have also discussed in Section 1.3 that in an optical trap, all spin components can be trapped. In fact, spins of atoms can play very important roles in two-body collisions, and their roles are different between the zero magnetic field limit and the finite magnetic field regime. In the zero magnetic field limit, the spin rotational symmetry is preserved, and the spin rotational symmetry imposes constraints on the form of two-body interactions, which will be discussed in this section. In the finite magnetic field regime, the spin rotational symmetry is broken by the Zeeman energy, but the Zeeman energy of spins can be used as a tool to tune the two-body interactions, which will be discussed in Section 2.4.

Alkali-Metal Atoms. Let us first consider the collision between two alkali-metal atoms with spin-f [2]. Here the spin refers to the total hyperfine spin. For simplicity, we take bosons with $f = 1$ as an example, which includes examples like the ground state of ^{87}Rb and ^{23}Na atoms. Due to the spin rotational symmetry, the total spin F of two atoms under collision should be conserved, and for the $f = 1$ case, the total spin of two atoms can therefore be either 0, 1, or 2. Thus, the interaction potential can be written in a diagonal form in the total spin bases as

$$\hat{V}(\mathbf{r}) = \frac{2\pi\hbar^2}{\bar{m}}(a_0\mathcal{P}_0 + a_2\mathcal{P}_2)\delta(\mathbf{r})\partial_r \cdot r, \tag{2.32}$$

where a_0 and a_2 denote the scattering length in the $F = 0$ and $F = 2$ channels, respectively. Here the $F = 1$ channel does not enter the s-wave scattering because the spin wave function is antisymmetric for total spin $F = 1$, and therefore the spatial wave function also has to be antisymmetric in order for the total wave function to be symmetric. Thus, the s-wave scattering is forbidden in this channel.

[2] Here we use little f to denote the spin of a single atom and capital F to denote the total spin of two atoms.

https://doi.org/10.1017/9781108595216.003 Published online by Cambridge University Press

The projection operator $\mathcal{P}_{\mathrm{F}}$ is to project the spin wave function of two atoms into subspace with total spin being F. To write $\mathcal{P}_{\mathrm{F}}$ more explicitly, say, in terms of physical observables, we can make use of the following two identities. First, by definition, the identity operator can be written as

$$\sum_{\mathrm{F}} \mathcal{P}_{\mathrm{F}} = 1. \tag{2.33}$$

Second, we consider $\mathbf{f}_1 \cdot \mathbf{f}_2$, and because $\mathbf{f}_1 \cdot \mathbf{f}_2 = (\mathbf{F}^2 - \mathbf{f}_1^2 - \mathbf{f}_2^2)/2$, $\mathbf{f}_1 \cdot \mathbf{f}_2$ only depends on F as

$$\mathbf{f}_1 \cdot \mathbf{f}_2 = \sum_F \left(\frac{F(F+1)}{2} - f(f+1) \right) \mathcal{P}_{\mathrm{F}}. \tag{2.34}$$

By further projecting both sides of Eq. 2.33 and Eq. 2.34 into the Hilbert space of symmetric total spin wave function, the term $\mathcal{P}_1$ can be dropped out. Therefore we have

$$\mathcal{P}_0 + \mathcal{P}_2 = 1 \tag{2.35}$$

$$-2\mathcal{P}_0 + \mathcal{P}_2 = \mathbf{f}_1 \cdot \mathbf{f}_2. \tag{2.36}$$

By solving these two equations, one can then express $\mathcal{P}_0$ and $\mathcal{P}_2$ in terms of identity operator and $\mathbf{f}_1 \cdot \mathbf{f}_2$, and one obtains [70, 130]

$$\hat{V}(\mathbf{r}) = \frac{2\pi\hbar^2}{\bar{m}} \left(a^{(\mathrm{n})} + a^{(\mathrm{s})} \mathbf{f}_1 \cdot \mathbf{f}_2 \right) \delta(\mathbf{r}) \partial_r \cdot r, \tag{2.37}$$

where

$$a^{(\mathrm{n})} = \frac{a_0 + 2a_2}{3} \tag{2.38}$$

$$a^{(\mathrm{s})} = \frac{a_2 - a_0}{3}. \tag{2.39}$$

Here $a^{(\mathrm{n})}$ and $a^{(\mathrm{s})}$ represent the density–density interaction and the spin-dependent interaction, respectively, and the latter is proportional to the difference in the scattering lengths between the $F = 0$ and $F = 2$ channels. When $a_0 = a_2$, the interactions are identical for different spin channels, and therefore $a^{(\mathrm{s})}$ vanishes. In this case, the interaction only depends on the total density, which is invariant under an arbitrary $SU(3)$ rotation of all three spin components. Therefore, the Hamiltonian is $SU(3)$ invariant instead of $SU(2)$ invariant.

Here we should also emphasize that one needs to carefully distinguish the high-spin representation of $SU(2)$ symmetry and the basic representation of $SU(N)$ symmetry. For the $SU(2)$ symmetry, there are only three generators, no matter how large S is, and the interaction is invariant under the rotation generated by these three generators. In the spin-S representation, these three generators are represented by $(2S+1) \times (2S+1)$ Pauli matrices. But for $SU(N)$ symmetry, there are in total N^2-1 generators, and the interaction is invariant under the rotation generated by all these $N^2 - 1$ generators.

In reality, for atoms like ^{87}Rb and ^{23}Na, the differences between a_0 and a_2 are actually quite small, and consequently, $a^{(\mathrm{s})}$ is only a few percent of $a^{(\mathrm{n})}$. Nevertheless, $a^{(\mathrm{s})}$ plays an important role for spin-1 alkali-metal atoms. Dynamically, this spin-dependent interaction

https://doi.org/10.1017/9781108595216.003 Published online by Cambridge University Press

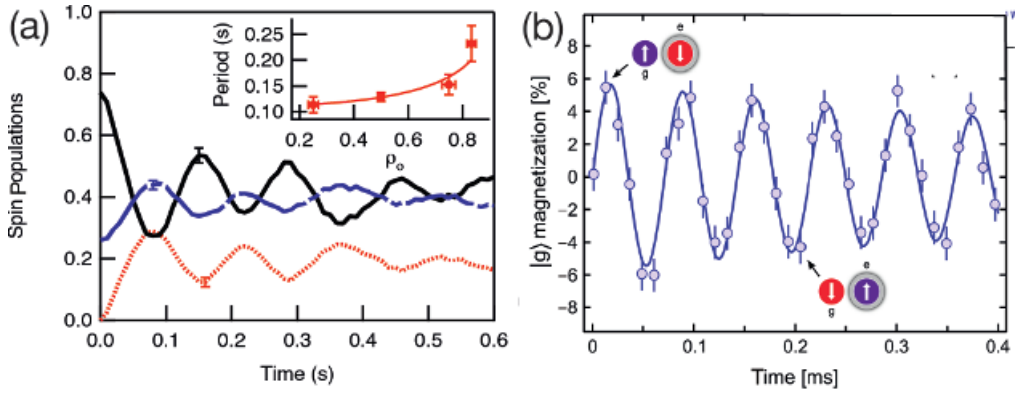

Figure 2.4 Interaction-induced spin exchanging dynamics. (a) The spin exchanging dynamics for spin-1 ^{87}Rb atom. The solid, dotted, and dashed lines are populations on $m_f = 0, 1$, and -1, respectively. Reprinted from Ref. [30]. (b) The nuclear spin exchanging between $|g\rangle$ and $|e\rangle$ states for ^{173}Yb atom. This line is a time-dependent nuclear spin polarization for atoms in $|g\rangle$ state, that is, the population difference between $|g\rangle|\uparrow\rangle$ and $|g\rangle|\downarrow\rangle$. Reprinted from Ref. [27]. A color version of this figure can be found in the resources tab for this book at cambridge.org/zhai.

can lead to a spin exchanging process. Because there are terms $f_1^+ f_2^- + f_1^- f_2^+$ in $\mathbf{f}_1 \cdot \mathbf{f}_2$, two incoming atoms with $f_z = 0$ can be scattered into one in $f_z = 1$ and the other in the $f_z = -1$ state. This process has been observed experimentally, and one of the examples is shown in Figure 2.4(a). Moreover, $a^{(s)}$ determines the spin structure of the Bose–Einstein condensate of spin-1 atoms, as we will see in Section 4.3.

Alkaline-Earth-Metal Atoms. As we have discussed in Section 1.1, for the ground state, the spin of alkaline-earth-metal atoms is purely nuclear spin I. Because the electron spin is zero, there is no coupling between the nuclear spin and the electronic degree of freedom. The nuclear spin is nonzero only for the fermionic alkaline-earth-metal atom because all the bosonic isotopes of alkaline-earth-metal atoms have zero nuclear spin. On the other hand, for fermionic isotopes, the nuclear spin usually can be quite large, and because of the decoupling between the nuclear spin and the electronic degree of freedom, the interaction between two ground-state alkaline-earth-metal atoms is nearly independent of nuclear spin I [193]. Therefore, all the scattering lengths between any two components are all identical, and the interaction only depends on the total density. Such an interaction term possesses $SU(2I + 1)$ symmetry.

Another interesting aspect of alkaline-earth-metal atoms is the interaction between the ground state $^1S_0$ (usually denoted by $|g\rangle$) and the clock state $^3P_0$ (usually denoted by $|e\rangle$). As discussed in Section 1.1, the clock state has long enough lifetime whose single-particle decay can be safely ignored in practice. In literature, these two states are also referred to as a doublet of the "orbital" degree of freedom.[3] Here we consider the interaction between two fermionic alkaline-earth-metal atoms, one in $|g\rangle$ state and the other in $|e\rangle$ state, and

[3] Note that here "orbital" labels an internal degree of freedom for atoms, that is, one of the valance electrons is excited to the excited p-orbit.

https://doi.org/10.1017/9781108595216.003 Published online by Cambridge University Press

they can be in two (among $2I+1$) different nuclear spin states, denoted by $|\uparrow\rangle$ and $|\downarrow\rangle$, respectively. Because the total wave function has to be antisymmetric, and because we consider the s-wave interaction that requires spatial wave function to be symmetric, the internal wave function has to be antisymmetric, which limits the internal Hilbert space to either the orbital triplet and the nuclear spin singlet or the orbital singlet and the nuclear spin triplet, which are

$$|+\rangle = \frac{1}{2}\left(|g\rangle|e\rangle + |e\rangle|g\rangle\right) \otimes \left(|\uparrow\rangle|\downarrow\rangle - |\downarrow\rangle|\uparrow\rangle\right), \tag{2.40}$$

$$|-,0\rangle = \frac{1}{2}\left(|g\rangle|e\rangle - |e\rangle|g\rangle\right) \otimes \left(|\uparrow\rangle|\downarrow\rangle + |\downarrow\rangle|\uparrow\rangle\right), \tag{2.41}$$

$$|-,1\rangle = \frac{1}{\sqrt{2}}\left(|g\rangle|e\rangle - |e\rangle|g\rangle\right) \otimes |\uparrow\rangle|\uparrow\rangle, \tag{2.42}$$

$$|-,-1\rangle = \frac{1}{\sqrt{2}}\left(|g\rangle|e\rangle - |e\rangle|g\rangle\right) \otimes |\downarrow\rangle|\downarrow\rangle, \tag{2.43}$$

where $\pm$ refers to orbital triplet and singlet, respectively, and $0, \pm 1$ in Eq. 2.41–2.43 refers to the z-component of the total nuclear spin. Here we have ignored two orbital triplet states where both atoms are in ground states or both atoms are in the clock state, because here we are interested in the interorbital interaction.

Above we have discussed that the interactions between atoms in the ${}^1S_0$ state have $SU(2I+1)$ symmetry. For atoms in the clock state ${}^3P_0$, because the total electronic angular momentum is also zero, the nuclear spin is still decoupled from the electronic degree of freedom, and therefore the interorbital interactions between the ${}^1S_0$ state and ${}^3P_0$ state also possess the $SU(2I+1)$ symmetry. Here, if we only consider two out of $2I+1$ nuclear spin components, the interactions possess an $SU(2)$ nuclear spin rotational symmetry. On the other hand, because the "orbital" degree of freedom is just a label of two different states, which is similar to the pseudo-spin-1/2 discussed in Box 2.3, there is no rotational symmetry requirement in the orbital space. This symmetry requirement leads to the following: (1) the interaction is diagonal in the bases of Eq. 2.40–2.43 listed above and (2) the $|+\rangle$ channel has one scattering length, and all three $|-\rangle$ channels share another different scattering length.

Denoting $\mathcal{P}_+$ as projection operator to $|+\rangle$ state, and $\mathcal{P}_-$ as projection operator to the Hilbert space spanned by three $|-\rangle$ ($m_n = 0, \pm 1$) states, we have

$$\mathcal{P}_+ = |+\rangle\langle+| \tag{2.44}$$

$$\mathcal{P}_- = |-,0\rangle\langle-,0| + |-,-1\rangle\langle-,-1|, +|-,+1\rangle\langle-,+1|. \tag{2.45}$$

The interaction can be written as

$$\hat{V}(\mathbf{r}) = \frac{2\pi\hbar^2}{\bar{m}}\left(\sum_{\pm} a_{\pm}\mathcal{P}_{\pm}\right)\delta(\mathbf{r})\partial_r \cdot r, \tag{2.46}$$

where $a_\pm$ are two different scattering lengths. For this interaction form, when one atom in $|g\rangle|\uparrow\rangle$ state collides with another atom in $|e\rangle|\downarrow\rangle$ state, there is a channel in which the outcoming atoms are one in $|g\rangle|\downarrow\rangle$ state and the other in $|e\rangle|\uparrow\rangle$ state. In other words,

https://doi.org/10.1017/9781108595216.003 Published online by Cambridge University Press

Box 2.3 Spin and Spin Rotational Symmetry

In ultracold atom literatures, "spin" can have different meanings. In some cases, spin means the total hyperfine spin of an atom, as discussed in this section and in spinor condensate discussed in Section 4.3. In such cases, interaction between different spin components should obey the spin rotational symmetry at zero field. In this case, the accuracy of the spin rotational symmetry is guaranteed by the fact that the collision energy between two atoms is much weaker compared with the hyperfine coupling of a single atom.

In some other cases, spin actually means the pseudo-spin, which are essentially two or more eigenstates of the total spin Hamiltonian, including both hyperfine coupling and the Zeeman field, as discussed in Section 1.2. In such cases, it is not necessary for interactions between different pseudo-spin components to obey the spin rotational symmetry. In this context, we can have pseudo-spin-$1/2$ Bose gas, which is not possible with real spins. For pseduo-spin-$1/2$ bosons, the two intracomponent interaction parameters and the intercomponent interaction parameter can in principle take arbitrary values. Therefore, there is no spin $SU(2)$ symmetry. The spin-orbit coupled Bose condensate discussed in Section 4.5 is such an example.

For pseudo-spin-$1/2$ Fermi gas, at the lowest order, there are intercomponent s-wave interactions and two intracomponent p-wave interactions, because the intracomponent s-wave interactions vanish due to the Fermi statistics. In general, the two intracomponent p-wave interactions are different, especially when one of them possesses a p-wave Feshbach resonance. However, away from the high-partial wave Feshbach resonances, the high-partial wave interaction can be safely ignored at ultra low temperature compared with the s-wave interaction, as discussed in Section 2.1, and we only need to retain the intercomponent interaction. Under this situation, the interaction again possesses an emergent $SU(2)$ symmetry. In this case, the accuracy of this emergent $SU(2)$ symmetry is guaranteed by the fact that the high-partial wave interaction energy is much weaker compared with the intercomponent s-wave interaction. The spin-$1/2$ Fermi gas discussed in Part III of this book, as well as the Fermi–Hubbard model discussed in Section 8.2, belongs to this case. In particular, we will emphasize the role of the $SU(2)$ spin rotational symmetry in the discussion of the Fermi–Hubbard model.

the nuclear spin between two different orbital states can be exchanged during the collision. This spin exchanging interaction strength is proportional to the difference between a_+ and a_-. This spin exchanging processes have also been observed in experiments [152, 27], as shown in Figure 2.4(b).

Such a spin-exchanging process can find broad applications in quantum simulation of many-body physics, for instance, in simulating the famous Kondo physics with ultracold atoms. The Kondo physics in condensed matter system arises from a localized magnetic impurity embedded in metal, and this magnetic impurity can exchange spin with itinerant electrons. Here, because the scalar polarizabilities are different between atoms in the $|g\rangle$ state and atoms in the $|e\rangle$ state, with the optical lattice scheme discussion in Section 1.3, one can create a situation that atoms in $|e\rangle$ state are localized by a deep potential, and atoms in $|g\rangle$ state experience a shallow potential and remain itinerant [62, 190, 149]. Thus, the atoms in $|e\rangle$ state act as localized impurities embedded in a Fermi sea of the itinerant atoms

https://doi.org/10.1017/9781108595216.003 Published online by Cambridge University Press

in $|g\rangle$ state, and the spin exchanging interaction between them can realize the Kondo effect [62, 190].

2.4 Feshbach Resonance

The discussion in Section 2.1 has established that the scattering length is an important quantity for describing the interatomic interaction. Can we tune the scattering length experimentally? In Section 2.1, using the square well potential as an example, we have also shown that the scattering length can be changed by changing the depth of a square well potential. However, in practice, it is hard to vary the strength of the Van der Waals potential over a large energy range. Nevertheless, the discussion in Section 2.1 gives an important hint, that is, if one can tune the energy of a bound state to be close to the scattering threshold, it can strongly affect the scattering length. This is essentially the key idea behind all tunable scattering resonances. Here we should first discuss a magnetic field–tunable *Feshbach resonance*.

The discussion of magnetic Feshbach resonance involves the internal spin structure of atoms in a magnetic field. We should recall that in Section 2.3, we have discussed the role of internal spin structure for two-body collision. The difference between the discussion here and that in Section 2.3 is that here we consider the regime where the effect of an external Zeeman field is strong enough. In Section 2.3 we focus on the zero-field regime where the spin rotational symmetry plays an important role, and we have discussed how the spin rotational symmetry imposes constraints on the form of interaction. But here the presence of a finite Zeeman field breaks the spin rotational symmetry, and therefore such a constraint no longer exists.

Now let us be more specific. We consider interaction between two alkali-metal atoms whose internal spin structure in a Zeeman field has been discussed in Sec 1.2. Let us label each internal spin eigenstate of a single atom in a Zeeman field by $|q\rangle$, which has a well-defined quantum number F_z. For instance, for ^{6}Li, the internal spin eigenstates are shown in Figure 2.5(b). Though there is no $SU(2)$ spin rotational symmetry because of the Zeeman field, there is still a spin rotational symmetry along the field direction, and thus F_z is still a good quantum number. When two atoms are far from each other, they are in the eigenstate of $|q_1\rangle \otimes |q_2\rangle$. Now we can introduce the concepts of two scattering channels. One is the called the *open channel* and the other is called the *closed channel*. These channels are defined as eigenstates when two atoms are far separated. Here are a few remarks about these two channels:

- Quantum Number: Due to the rotational symmetry along $\hat{z}$, the total $F_z^1 + F_z^2 + L_z$ is conserved. Here $F_z^{i=1,2}$ is the z-component of the hyperfine spin of these two atoms, respectively, and L_z is the $\hat{z}$-component of their relative angular momentum. Here, for simplicity, we only consider the s-wave states in both the open and the closed channels, and $L_z = 0$. With this simplification, the total $F_z^1 + F_z^2$ of the open channel should equal to that of the closed channel. For instance, for ^{6}Li, if the open channel is taken as $|a\rangle \otimes |b\rangle$

https://doi.org/10.1017/9781108595216.003 Published online by Cambridge University Press

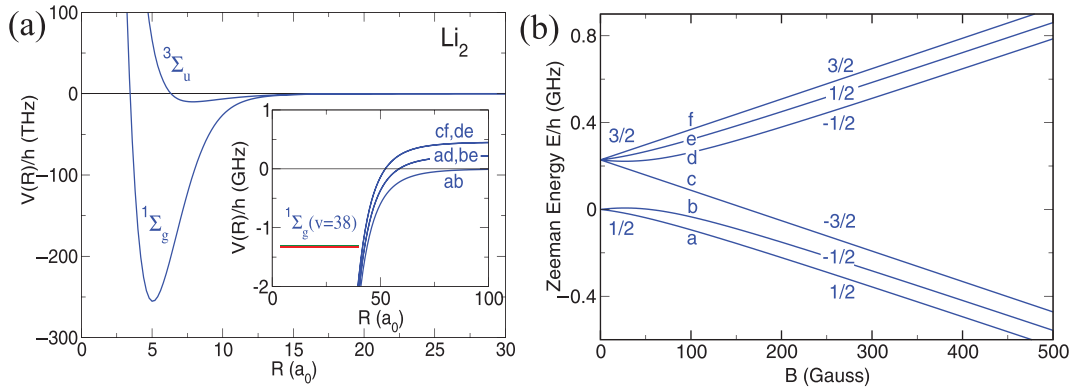

Figure 2.5 Interaction channels between two alkali-metal atoms. (a) The electronic spin singlet and triplet interaction potential of Li_2 at short interatomic separation. The inset shows a zoom-in plot of the interaction potential of two ^{6}Li atoms at large interatomic separation. The five pairs of states all have total $F_z = 0$. The horizontal line shows a bound state in the closed channel. (b) The internal eigenstate labeled from *a* to *f* of ^{6}Li. The number on each curve is the value of F_z for each state. Reprinted from Ref. [34]. A color version of this figure can be found in the resources tab for this book at cambridge.org/zhai.

with total $F_z = 0$, there are in total five combinations that have total $F_z = 0$, and the other four are $|a\rangle \otimes |d\rangle$, $|b\rangle \otimes |e\rangle$, $|c\rangle \otimes |f\rangle$, and $|d\rangle \otimes |e\rangle$.

- Closed versus Open: When two atoms are far separated, the energy difference between the open and the closed channel is set by the Zeeman energy, which is normally much higher than the kinetic energy. Therefore, when two atoms collide from the low-energy scattering state of the open channel, they cannot be scattered into scattering states of the closed channel. That is why these channels are called "closed channels." As shown in the inset of Figure 2.5(a), all the other four combinations can be taken as closed channels when $|a\rangle \otimes |b\rangle$ is chosen as the open channel.
- Energy Tunability: Usually when the open channel is chosen as the low-lying hyperfine spin state, as the magnetic field increases, the energy of the open channel decreases with respect to the closed channel. Thus, it is conceivable that, as magnetic field increases, the scattering threshold can approach a bound state in the closed channel from above.
- Coupling between Channels: When two atoms are close to each other, the inter-atomic potential between two atoms mostly depends on the electronic degree of freedom of two atoms. Here, since each alkali-metal atom has one electron, the interatomic potential depends on whether their total electronic spin is singlet or triplet,[4] an example of which is shown in Figure 2.5(a). For instance, considering the open channel $|a\rangle \otimes |b\rangle$, their electron spins are polarized by the magnetic field, and their total electronic spin is more close to a triplet. However, the hyperfine coupling mixes in electron spin singlet

[4] In practice, the Van der Waals part is the same for electron spin singlets and triplets, but the short-range repulsive part depends on electron spin.

https://doi.org/10.1017/9781108595216.003 Published online by Cambridge University Press

component. Hence, the short-range potential couples different channels, though the coupling is usually weak.

Coupled-Channel Model. With these features of the two channels discussed above, we can consider a simplified coupled-channel model to demonstrate how the scattering length can be changed by the magnetic field [34]. The model is schematically illustrated in Figure 2.6(a). The major considerations are as follows:

- At the distance $r > r_0$, two channels are decoupled, and they are respectively denoted by the open channel $|o\rangle$ and the closed channel $|c\rangle$. Because the energy of the closed

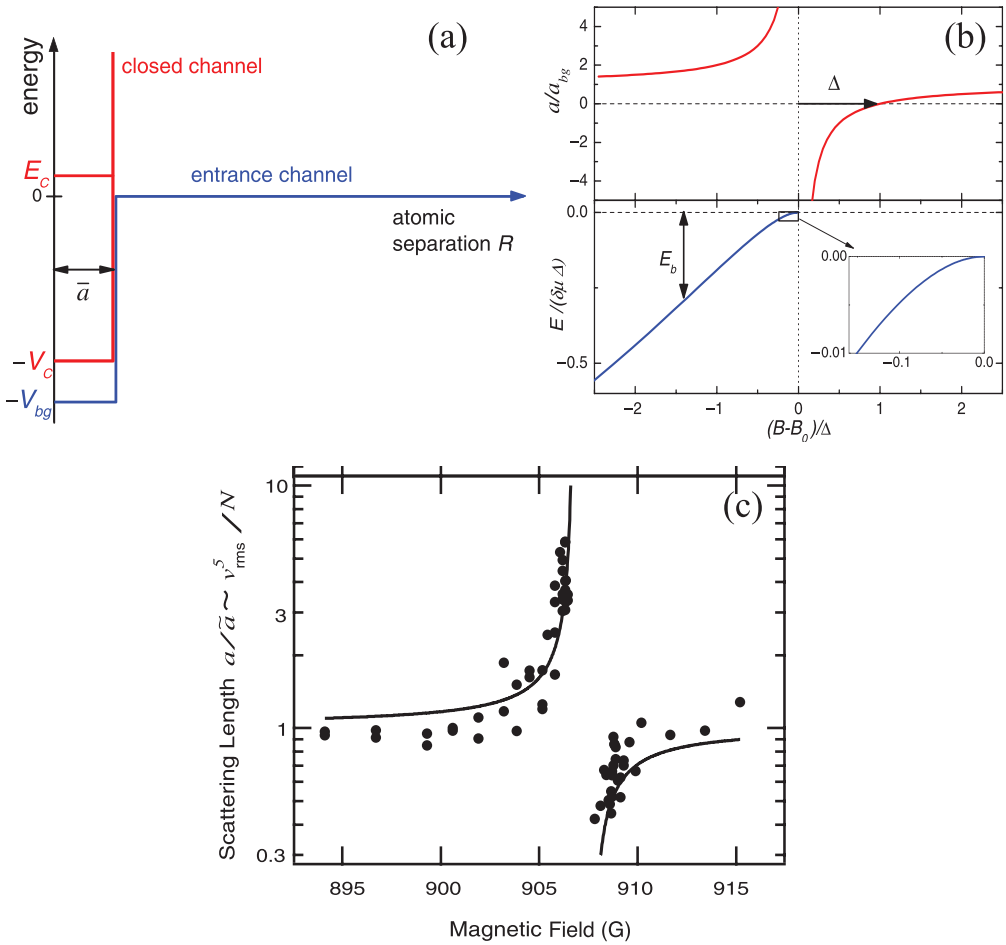

Figure 2.6 Feshbach resonance. (a) A schematic of the simplified two-channel model. (b) The magnetic field dependence of the scattering length and the bound state energy, where B_0 is B_{res} in the text. (c) The first experimental observation of a Feshbach resonance in ^{23}Na. (a) and (b) are reprinted from Ref. [34], and (c) is reprinted from Ref. [79]. A color version of this figure can be found in the resources tab for this book at cambridge.org/zhai.

https://doi.org/10.1017/9781108595216.003 Published online by Cambridge University Press

channel is much higher than the typical kinetic energy of incoming scattering states of the open channel, the wave function of low-lying scattering states only exists in the open channel $|o\rangle$, and the low-energy s-wave wave function is given by $\Psi = \chi/r$ and

$$\chi = \sin(kr + \delta_k)|o\rangle. \tag{2.47}$$

- At the distance $r < r_0$, the wave function is diagonalized in the $|+\rangle$ and $|-\rangle$ bases, written as

$$\chi = \chi_+|+\rangle + \chi_-|-\rangle. \tag{2.48}$$

Here $|\pm\rangle$ are superposition of $|o\rangle$ and $|c\rangle$ as

$$|+\rangle = \cos\theta|o\rangle + \sin\theta|c\rangle \tag{2.49}$$

$$|-\rangle = -\sin\theta|o\rangle + \cos\theta|c\rangle. \tag{2.50}$$

Without loss of generality, we consider θ as spatially independent and quite small.

The wave function in the $r < r_0$ regime can now be written as

$$\chi = (\chi_+ \sin\theta + \chi_- \cos\theta)|c\rangle + (\chi_+ \cos\theta - \chi_- \sin\theta)|o\rangle. \tag{2.51}$$

To match the boundary conditions in $r = r_0$, we obtain

$$\chi_+ \sin\theta + \chi_- \cos\theta\Big|_{r=r_0} = 0 \tag{2.52}$$

$$\frac{\chi'_+ \cos\theta - \chi'_- \sin\theta}{\chi_+ \cos\theta - \chi_- \sin\theta}\Big|_{r=r_0} = \frac{k}{\tan\delta_k} \equiv -\frac{1}{a_s}. \tag{2.53}$$

Eq. 2.52 comes from that the closed channel wave function vanishes at $r = r_0$, and Eq. 2.53 determines the phase shift in the open channel scattering wave function. As discussed in Section 2.1, here we have assumed that both $\chi_\pm$ is independent of energy and r_0 is a small value. These two equations give

$$-\frac{1}{a_s} = \frac{\chi'_+}{\chi_+}\Big|_{r=r_0} \cos^2\theta + \frac{\chi'_-}{\chi_-}\Big|_{r=r_0} \sin^2\theta. \tag{2.54}$$

Since θ is usually quite small, the second term on the r.h.s. of Eq. 2.54 is usually insignificant. In that case, the scattering length is provided by the $|+\rangle$ channel only, and we denote

$$\frac{\chi'_+}{\chi_+}\Big|_{r=r_0} = -\frac{1}{a_{bg}}, \tag{2.55}$$

where a_{bg} is called the background scattering length. Now we have

$$-\frac{1}{a_s} = -\frac{1}{a_{bg}} \cos^2\theta + \frac{\chi'_-}{\chi_-}\Big|_{r=r_0} \sin^2\theta. \tag{2.56}$$

Again because θ is small, we can approximate $\cos^2\theta \approx 1$ and $\sin^2\theta \approx \theta^2$, and the second term can give rise to a significant contribution only when $\chi'_-/\chi_-|_{r=r_0}$ is very large. As we

https://doi.org/10.1017/9781108595216.003 Published online by Cambridge University Press

will see, this means nothing but a bound state appearing nearby the threshold in the $|-\rangle$ channel.

For instance, let us consider the $|-\rangle$ channel as a square well with $V(r) = -V_0$ ($V_0 > 0$) for $r < r_0$, as shown in Figure 2.6(a). In this case, when the energy of the scattering state can be ignored compared with V_0, we have $\chi_- = \sin(q_1 r)$ and $q_1 = \sqrt{mV_0/\hbar^2}$, therefore,

$$\left.\frac{\chi_-'}{\chi_-}\right|_{r=r_0} = \frac{q_1 \cos(q_1 r_0)}{\sin(q_1 r_0)}. \tag{2.57}$$

If there is a bound state with energy E_c, then the bound state wave function is $\chi_-(r) = \sin(q_2 r)$ and $q_2 = \sqrt{m(V_0 + E_c)/\hbar^2}$, and to zeroth order of θ, $|-\rangle$ channel connects to $|c\rangle$ channel at $r = r_0$ and $\sin(q_2 r_0) = 0$. When E_c is small, we can expand q_1 around q_2 and obtain

$$\left.\frac{\chi_-'}{\chi_-}\right|_{r=r_0} \approx \frac{q_1}{(q_1 - q_2) r_0} \approx \frac{2q_1^2}{(q_1^2 - q_2^2) r_0} = -\frac{2\hbar^2 q_1^2}{m r_0 E_c}. \tag{2.58}$$

In fact, although we derive Eq. 2.58 using a square well potential, it holds for a general potential that $\chi_-'/\chi_-|_{r=r_0}$ is inversely proportional to E_c. Denoting $\gamma = 2\hbar^2 q_1^2 \theta^2/(m r_0)$, Eq. 2.56 can be rewritten as

$$\frac{1}{a_s} = \frac{1}{a_{bg}} + \frac{\gamma}{E_c}. \tag{2.59}$$

Here it is important to note that γ depends on θ, which is the coupling between two channels. Eq. 2.59 gives

$$a_s = a_{bg}\left(1 - \frac{\gamma a_{bg}}{E_c + \gamma a_{bg}}\right). \tag{2.60}$$

In the presence of a magnetic field, the threshold energies of the open and the closed channel change as $-\mu_o B$ and $-\mu_c B$, respectively. In most cases, $\mu = \mu_o - \mu_c > 0$. E_c is replaced by $E_c - \mu_c B + \mu_o B = E_c + \mu B$. Defining $\Delta = \gamma a_{bg} \mu^{-1}$ and $B_{res} = -\mu^{-1} E_c - \Delta$, Eq. 2.60 can be rewritten as

$$a_s = a_{bg}\left(1 - \frac{\Delta}{B - B_{res}}\right). \tag{2.61}$$

This result shows that, usually for $\mu > 0$, a_s diverges to $+\infty$ when $B \to B_{res}$ from below and diverges to $-\infty$ when $B \to B_{res}$ from above, as shown in Figure 2.6(b). B_{res} denotes the magnetic field for a scattering resonance, which is close to the position with $E_c = 0$ but is shifted away by Δ. Δ defines the width of a resonance. From Eq. 2.61, one can see that $a_s = \infty$ when $B = B_{res}$ and $a_s = 0$ when $B = B_{res} + \Delta$, and the latter is known as the zero crossing. Thus, Δ measures the distance between the magnetic field for resonant scattering and the magnetic field for the zero crossing. Figure 2.6(c) shows the first experimental observation of a Feshbach resonance in ^{23}Na [79]. Later Feshbach resonances are found in almost all alkali-metal and magnetic atoms, which have become the most important tools for controlling interaction in ultracold atomic physics.

https://doi.org/10.1017/9781108595216.003 Published online by Cambridge University Press

Wide versus Narrow Resonance. One can further show that at finite energy,

$$a_s(E) = a_{bg}\left(1 - \frac{\mu\Delta}{\mu(B - B_{res}) - E}\right). \tag{2.62}$$

Expanding $-1/a_s(E) = -1/a_s + r_{eff}k^2/2$, with $E = \hbar^2k^2/m$, one obtains the effective range as

$$r_{eff} = -\frac{2\hbar^2\Delta}{\mu m a_{bg}(B - B_{res} - \Delta)^2} \approx -\frac{2\hbar^2}{\mu\Delta m a_{bg}}, \tag{2.63}$$

where the second approximate equality is valid nearby the resonance. This equation shows that the effective range depends on Δ; that is, it depends on γ or θ. This is a major difference between the single-scattering channel model discussed in Section 2.1 and the two-channel model discussed here. In the single-channel model, as discussed in Section 2.1, one can also fine-tune the potential such that there is a bound state at the threshold, and such a resonance is also called a *shape resonance*. Usually for an *s*-wave shape resonance, r_{eff} is usually negligible. But for the two-channel model, depending on how strong the mixing between the open and the closed channel is, the effective range can be tuned over a wide range from very small to quite large, and the sign of r_{eff} depends on the sign of a_{bg}. That is to say, only when Δ in the Feshbach resonance is large enough that r_{eff} is sufficiently small, a Feshbach resonance in the two-channel model is equivalent to a shape resonance in a single-channel model. To characterize the role of the effective range in a many-body system of degenerate Fermi gas, a dimensionless quantity $k_F r_{eff}$ is introduced as

$$k_F r_{eff} = \frac{4E_F}{\mu\Delta(k_F a_{bg})}. \tag{2.64}$$

If $k_F r_{eff} \ll 1$, we call it a *wide resonance*, and if $k_F r_{eff} \gg 1$, we call it a *narrow resonance*. For a narrow resonance, effectively, the scattering length varies a lot over the energy range of E_F; thus the many-body system cannot be described by a single energy-independent parameter of the scattering length a_s. In Chapters 5 and 6, when we discuss the many-body physics of ultracold Fermi gases across a Feshbach resonance, we focus on the wide resonances.

Zero-Range Two-Channel Model. In Section 2.2, we have introduced a zero-range model to describe a single-channel scattering problem. We emphasize that a renormalization condition has to be introduced in order to remove the artificial short-range divergency when taking the range of potential to zero. Above we have introduced a coupled two-channel scattering problem, and we have also noted that the two-channel model is not always equivalent to the single-channel model when the energy dependence of the scattering length has to be taken into account for narrow resonances. Hence, it is desirable to introduce a zero-range version of the two-channel model, which can describe both the wide and the narrow Feshbach resonances. As we will see, here we also need to be careful about the renormalization of the model parameters.

Here, similarly to in Section 2.2, we consider two-component fermions as an example. To capture the two-channel nature of the problem, we explicitly introduce a bosonic $\hat{b}$

https://doi.org/10.1017/9781108595216.003 Published online by Cambridge University Press

field to describe the two-body bound state in the closed channel, which is also called the molecular state. Now the Hamiltonian is written as

$$\begin{aligned}\hat{\mathcal{H}} = &\sum_{\mathbf{k}\sigma} \frac{\hbar^2\mathbf{k}^2}{2m}\hat{\Psi}_{\mathbf{k}\sigma}\hat{\Psi}_{\mathbf{k}\sigma} + \sum_{\mathbf{k}}\left(\frac{\hbar^2\mathbf{k}^2}{4m} + \nu\right)\hat{b}^\dagger_{\mathbf{k}}\hat{b}_{\mathbf{k}} \\ &+ \frac{g}{V}\sum_{\mathbf{k},\mathbf{k_1},\mathbf{k_2}} \hat{\Psi}^\dagger_{\frac{\mathbf{k}}{2}+\mathbf{k}_{1,\uparrow}}\hat{\Psi}^\dagger_{\frac{\mathbf{k}}{2}-\mathbf{k}_{1,\downarrow}}\hat{\Psi}_{\frac{\mathbf{k}}{2}-\mathbf{k}_{2,\downarrow}}\hat{\Psi}_{\frac{\mathbf{k}}{2}+\mathbf{k}_{2,\uparrow}} \\ &+ \frac{\alpha}{\sqrt{V}}\sum_{\mathbf{k},\mathbf{k_1}} \hat{\Psi}^\dagger_{\frac{\mathbf{k}}{2}+\mathbf{k}_{1,\uparrow}}\hat{\Psi}^\dagger_{\frac{\mathbf{k}}{2}-\mathbf{k}_{1,\downarrow}}\hat{b}_{\mathbf{k}} + \hat{b}^\dagger_{\mathbf{k}}\hat{\Psi}_{\frac{\mathbf{k}}{2}-\mathbf{k}_{1,\downarrow}}\hat{\Psi}_{\frac{\mathbf{k}}{2}+\mathbf{k}_{1,\uparrow}},\end{aligned} \tag{2.65}$$

where $\hat{\Psi}^\dagger_\sigma$ and $\hat{\Psi}_\sigma$ are the creation and annihilation operators for scattering states in the open channels. The last term denotes the conversion between the open channel scattering states and the closed channel molecular state, with the strength given by α. Here ν is the detuning of the molecular state in the closed channel, and g is the bare interaction between open channel atoms themselves. This model is a zero-range model because both g and α are chosen as momentum independent. Here, for the reason discussed above, we do not include the scattering states in the closed channel. To find the renormalization relations for ν, α, and g, similarly to our calculation done in Section 2.2, we can sum over the ladder diagrams for the two-channel model to obtain the two-body scattering T-matrix. The ladder diagram for the two-channel model is shown in Figure 2.3(b), compared with the ladder diagrams in the single-channel model. Here we obtain the T_2 as

$$T_2(E) = \frac{g + \frac{|\alpha|^2}{E-\nu}}{1 - \left(g + \frac{|\alpha|^2}{E-\nu}\right)\frac{1}{V}\sum_{\mathbf{k}}\frac{1}{E-\hbar^2\mathbf{k}^2/(m)}}. \tag{2.66}$$

By comparing $T_2(E=0) = 4\pi\hbar^2 a_s/m$ with a_s given by Eq. 2.61, we can obtain the renormalization conditions that

$$\frac{1}{g} = \frac{m}{4\pi\hbar^2 a_{bg}} - \Lambda, \tag{2.67}$$

$$\frac{1}{\alpha} = \left(1 - \frac{4\pi\hbar^2 a_{bg}}{m}\Lambda\right)\sqrt{\frac{m}{4\pi\hbar^2 a_{bg}\mu\Delta}}, \tag{2.68}$$

$$\nu = \mu(B - B_{res}) + \frac{\Lambda}{1 - \frac{4\pi\hbar^2 a_{bg}}{m}\Lambda}\frac{4\pi\hbar^2 a_{bg}\mu\Delta}{m}, \tag{2.69}$$

where Λ denotes

$$\Lambda = \frac{1}{V}\sum_{\mathbf{k}}\frac{1}{\hbar^2\mathbf{k}^2/m}. \tag{2.70}$$

General Schemes of the Feshbach Resonance. From the discussion above, we can summarize the following three key ingredients in order to support a Feshbach resonance:

- For $r > r_0$, atoms stay in the single-particle eigenstates, and the different quantum numbers of the single-particle eigenstates define "channels."

https://doi.org/10.1017/9781108595216.003 Published online by Cambridge University Press

- The energy spacing between different channels can be tuned by an external parameter.
- The short-range potential at $r < r_0$ does not respect the good quantum number of the single-particle Hamiltonian and thus mixes different channels.

For the magnetic Feshbach resonance of alkali-metal atoms discussed above, these three conditions are satisfied as follows:

- The channel is defined in terms of the spin quantum number of a single atom in the presence of a magnetic field, that is, the eigenstate of both the hyperfine interaction and the Zeeman field.
- The energy splitting between two channels can therefore be tuned by the Zeeman energy.
- The short-range potential largely depends on the total electron spin of two atoms being singlet or triplet, which does not conserve the spin quantum number of the single atom.

In the same spirit, we can also have several different types of Feshbach resonance. One is the optical Feshbach resonance. Here we briefly introduce how the optical Feshbach resonance satisfies the three ingredients:

- For $r > r_0$, the atoms are labeled by the electronic quantum number of a single atom. Taking an alkali-metal atom as an example, for the open channel, two atoms are both in the $^2S_{1/2}$ ground state, and for the closed channel, one atom is still in the $^2S_{1/2}$ state and the other atom is in the excited $^2P_{1/2}$ state. Here we should note that, although there presents a laser field, the laser frequency is far detuned from the single-particle transition, and to very good approximation, the single-particle electronic states are not affected by the laser when two atoms are far separated.
- In the presence of light, and by rotating wave approximation as discussed in Section 1.3, the effective energy difference between two channels is the excitation energy subtracted by the single photon energy. Thus, the energy spacing between two channels can be tuned by the laser frequency. When the laser frequency is detuned to be resonant with a bound state energy in the closed channel, the bound state is effectively tuned to the threshold of the open channel, at which a scattering resonance occurs.
- Since the laser is tuned to be resonant with a bound state in the closed channel, the two channels are coupled by the laser at the short distance when the molecular wave function is concentrated.

The optical Feshbach resonances have great advantages that they can provide very fast temporal control and small spatial resolution control of interactions, because the laser can be turned on and off much more rapidly than the magnetic field, and the laser intensity can be varied on the spatial scale of less than 1 μm. However, the disadvantage is that the excited state (such as $^2P_{1/2}$ of alkali-metal atoms) usually has finite lifetime due to the spontaneous emission. The loss, as well as the heating due to the loss, can be quite significant, preventing the system from reaching equilibrium in the regime nearby a resonance. In fact, a better stratagem is to combine the optical control with the magnetic Feshbach resonance, such that one can take the advantages of temporal and spatial control and can also avoid the heating problem.

https://doi.org/10.1017/9781108595216.003 Published online by Cambridge University Press

Another example is the orbital Feshbach resonance in alkaline-earth-metal atom, which has been first theoretically predicted [189] and then experimentally observed in ^{173}Yb [133, 75] and in ^{171}Yb [18]. As we have seen, the electron spin plays an important role in the magnetic Feshbach resonance of alkali-metal atoms, because the short-range potentials are labeled by the total electronic spin singlet and triplet. Because the electron spin of the ground state ($^1S_0$) alkaline-earth-metal atom is zero, the short-range potentials do not have the choice of the total electron spin being singlet or triplet, and therefore, the mechanism for the magnetic Feshbach resonance in alkali-metal atoms does not hold for alkaline-earth-metal atoms. Nevertheless, let us recall that in Section 1.1, we have discussed that alkaline-earth-metal atoms have a long-lived clock state $^3P_0$, and in Section 2.3, we have discussed the collision between two different nuclear spin states ($|\uparrow\rangle$ and $|\downarrow\rangle$) of a fermionic alkaline-earth-metal atom, with one in the ground state ($^1S_0$ denoted by $|g\rangle$) and the other in the clock state ($^3P_0$ denoted by $|e\rangle$). In Section 2.3, we focus on the zero magnetic field limit, and here we consider the presence of finite magnetic field. One crucial fact is that the nuclear spin Landé g-factor for $|e\rangle$ state is slightly larger than that of the $|g\rangle$ state [20]. This is because, as we have discussed in Section 1.1, $^3P_0$ state possesses certain coupling to $^3P_1$ state through the hyperfine coupling, which can be further coupled to $^1P_1$ state. The small but finite coupling to the electronic spin gives rise to a slightly larger g-factor of $^3P_0$ compared with $^1S_0$ state. With this in mind, let us briefly introduce how these three conditions can be satisfied in alkaline-earth-metal atoms [191]:

- For $r > r_0$, atoms stay in the single-particle spin eigenstates in the presence of a magnetic field. Here, for the open channel, one atom stays in $|g\downarrow\rangle$ and the other atom stays in $|e\uparrow\rangle$, and the wave function under antisymmetrization reads

$$|o\rangle = \frac{1}{\sqrt{2}}\left(|g\downarrow\rangle|e\uparrow\rangle - |e\uparrow\rangle|g\downarrow\rangle\right). \tag{2.71}$$

  For the closed channel, one atom stays in $|g\uparrow\rangle$ and the other atom stays in $|e\downarrow\rangle$, and the wave function under antisymmetrization reads

$$|c\rangle = \frac{1}{\sqrt{2}}\left(|g\uparrow\rangle|e\downarrow\rangle - |e\downarrow\rangle|g\uparrow\rangle\right). \tag{2.72}$$

- As mentioned above, because the $|g\rangle$ state and $|e\rangle$ state have slightly different g-factors, the energy difference between the open and the closed channels can in principle be tuned by the magnetic field. However, also because this g-factor difference is quite small, the range of tunability is also rather small. Typically, changing the magnetic field by 1 gauss, the Zeeman energy between two channels changes about $2\pi\hbar \times 100$ Hz. Note that for alkali-metal atoms, for the same amount of magnetic field, the change of Zeeman energy between channels is about five orders of magnitude larger. With such limited Zeeman energy tunability, it is hard to access a bound state with an accessible magnetic field range in the laboratory. But fortunately, nature is very kind. For both ^{173}Yb and ^{171}Yb atoms, there exists quite a shallow bound state in the interaction potential, which can be accessed even with this narrow tunable energy window.
- As we discussed in Section 2.3, for the four states mentioned above, the short-range potential is diagonal in the bases labeled by $|+\rangle$ and $|-,0\rangle$, as shown in Eq. 2.40 and

https://doi.org/10.1017/9781108595216.003 Published online by Cambridge University Press

Eq. 2.41. Because $|+\rangle$ and $|-,0\rangle$ can be written as $(|o\rangle \pm |c\rangle)/\sqrt{2}$, respectively, this short-range potential mixes the open and the closed channels.

With these three conditions satisfied, a magnetic field–tunable Feshbach resonance can also be reached in the alkaline-earth-metal atoms. However, the role of electronic spin in the alkali-metal case is now replaced by the so-called *orbital* degree of freedom that labels ${}^1S_0$ and ${}^3P_0$. To highlight this difference, the new Feshbach resonance is named as the *orbital Feshbach resonance*. There is a major physical difference between the magnetic Feshbach resonance and the orbital Feshbach resonance. In the former, as we repeatedly emphasized, the energy difference between two channels is much larger than the kinetic energy such that the closed channel cannot be populated by scattering states. But for the latter, this energy difference is reduced by five orders of magnitude, and therefore it is no longer much larger than the kinetic energy. Hence, the so-called closed channel can be populated by low-energy scattering states in a many-body system, and it is no longer closed [189]. This difference can manifest significantly in a strongly interacting Fermi gas nearby these resonances [189, 191].

2.5 Confinement-Induced Resonance

When a strong one- or two-dimensional confinement potential is applied, such a geometric confinement can reduce a three-dimensional system to a quasi-two- or quasi-one-dimensional one. In this section, we will discuss how to deduce the effective interaction strength for scattering in lower dimensions, starting from the original three-dimensional scattering problem with confinement potentials. We will show that the effective interaction strength in lower dimensions can diverge even when the original s-wave scattering length in three dimensions is finite. This is known as the *confinement-induced resonance* [131].

Here, as an example, we consider the quasi-one-dimensional situation; that is, a strong harmonic trap in the transverse xy plane is applied to a three-dimensional system, and the system remains uniform along the $\hat{z}$ direction. Note that the center of mass and relative motions are still separable with the presence of a harmonic trap, and the Schrödinger equation for the relative motion between two atoms is written as

$$\left[\frac{\hat{p}_z^2}{2\bar{m}} + \frac{\hat{p}_x^2+\hat{p}_y^2}{2\bar{m}} + \frac{\bar{m}\omega_\perp^2(x^2+y^2)}{2} + V(\mathbf{r})\right]\Psi(\mathbf{r}) = E\Psi(\mathbf{r}) \tag{2.73}$$

where $V(\mathbf{r})$ is the interatomic potential. Similarly to discussion in Section 2.1, when $r > r_0$, we can ignore the interaction potential, and the wave function is determined by the free Hamiltonian. Note that the transverse mode has energy $(n_x + n_y + 1)\hbar\omega_\perp$ $(n_x, n_y \geqslant 0)$. Here we focus on the energy range $\hbar\omega_\perp < E < 2\hbar\omega_\perp$. In this energy range, if the atoms are in the lowest transverse mode, they can be in scattering state along the longitudinal direction. And if atoms are in the transverse excited states, they can only be in the bound state along the longitudinal direction. Hence, the general form of the wave function can be written as

https://doi.org/10.1017/9781108595216.003 Published online by Cambridge University Press

$$\Psi = (e^{ik_z z} + f_{\text{even}} e^{ik_z|z|})\varphi_0(x)\varphi_0(y) + \sum_{n_x+n_y\neq 0} \alpha_{n_x,n_y}\varphi_{n_x}(x)\varphi_{n_y}(y)e^{-\kappa_{n_x n_y}|z|}, \tag{2.74}$$

where $E = \hbar\omega_\perp + \hbar^2 k_z^2/(2\bar{m}) = \hbar\omega_\perp(n_x + n_y + 1) - \hbar^2\kappa_{n_x n_y}^2/(2\bar{m})$. Here f_{even} is the even parity scattering amplitude, and odd parity scattering amplitude vanishes because of the requirement of wave function continuity at $z = 0$. Here φ_n is the eigen-mode of a one-dimensional harmonic oscillator. Because the second term in the wave function Eq. 2.74 vanishes at large z, the asymptotic form of this scattering wave function is given by the first term as

$$\Psi(z,\rho) \to (e^{ik_z z} + f_{\text{even}} e^{ik_z|z|})\varphi_0(x)\varphi_0(y). \tag{2.75}$$

For $r < r_0$, the single-particle energy can be ignored, and the wave function is determined by the short-range interaction potential. Similarly, for the s-wave channel, we can match the boundary condition by requiring $(r\Psi)'/(r\Psi)\big|_{r=r_0} = -1/a_s$, and for a higher partial wave channel, we assume the interaction effects are negligible. Nevertheless, the difficulty here is that the short-range boundary condition is spherical symmetrical but the wave function Eq. 2.74 is cylindrical symmetrical. After some quite involved calculation using the frame transformation [187], one finally reaches [131]

$$f_{\text{even}}(k_z \to 0) = -\frac{1}{1 - \frac{ik_z a_\perp}{2}\left(\frac{a_\perp}{a_s} + \mathcal{C}\right)}, \tag{2.76}$$

where $a_\perp = \sqrt{\hbar/\bar{m}\omega}$ and $\mathcal{C} \approx -1.46$.

Next we consider a real one-dimensional case. We shall also model the one-dimensional scattering process in terms of a zero-range potential. Unlike the three-dimensional case, the one-dimensional wave function does not display any singularity when $z \to 0$, and therefore, a δ-function potential is regular in one dimension. Hence, we write down the Hamiltonian with δ-function interaction as

$$\left[-\frac{\hbar^2}{2\bar{m}}\frac{\partial^2}{\partial z^2} + g_{1\text{d}}\delta(z)\right]\Psi(z) = E\Psi(z). \tag{2.77}$$

When $z \neq 0$, the wave function of the kinetic energy eigenstate is generally written as

$$\Psi = e^{ik_z z} + f_{\text{even}} e^{ik_z|z|}, \tag{2.78}$$

where $E = \hbar^2 k_z^2/(2\bar{m})$. For a δ-function potential, we can use the continuity condition that $\Psi'(0^+) - \Psi'(0^-) = 2\bar{m}g_{1\text{d}}\Psi(0)/\hbar^2$ to determine f_{even}, which gives rise to

$$ik_z f_{\text{even}} = \frac{\bar{m}g_{1\text{d}}}{\hbar^2}(1 + f_{\text{even}}); \tag{2.79}$$

that is

$$f_{\text{even}} = -\frac{1}{1 - i\frac{\hbar^2}{\bar{m}g_{1\text{d}}}k_z}. \tag{2.80}$$

Introducing "one-dimensional scattering length" $a_{1\text{d}}$ as

$$g_{1\text{d}} = -\frac{\hbar^2}{\bar{m}a_{1\text{d}}}, \tag{2.81}$$

https://doi.org/10.1017/9781108595216.003 Published online by Cambridge University Press

we can write

$$f_{\text{even}} = -\frac{1}{1 + ika_{1\text{d}}}. \tag{2.82}$$

To determine the effective one-dimensional interaction scattering length $a_{1\text{d}}$, one requires that the scattering amplitude f_{even} obtained from the one-dimensional model Eq. 2.82 reproduce f_{even} of Eq. 2.76 obtained from the full three-dimensional calculation with confinement potential. As we emphasized at the beginning of this chapter, since the ultracold atomic systems are dilute and the typical interatomic separation is much larger than the range of potential, and the collision energy is also very small compared with the interaction potential, the interaction mostly manifests in the asymptotic wave function. Therefore, if these two situations give the same asymptotic wave functions, we consider this $g_{1\text{d}}$ as a faithful representation of the interaction in the reduced dimension. Hence, by matching Eq. 2.82 with Eq. 2.76, we obtain

$$\frac{a_{1\text{d}}}{a_\perp} = -\frac{1}{2}\left(\frac{a_\perp}{a_{\text{s}}} + \mathcal{C}\right). \tag{2.83}$$

This shows that when $a_\perp/a_{\text{s}} = -\mathcal{C}$, $a_{1\text{d}} = 0$ and $g_{1\text{d}}$ diverges, which is known as the confinement-induced resonance [131].

Although the discussion of the confinement-induced resonance appears quite different from the discussion of Feshbach resonance in Section 2.4, it can be essentially understood in the same way as a Feshbach resonance [17]. In Section 2.4, we established three points as the key ingredients for a Feshbach resonance, and here we can show that the confinement-induced resonance can also be understood in terms of these three points.

- When two atoms are separated, atoms stay in the single-particle eigenstates. Here we use different eigenstates in the transverse direction to label "channels." For the open channel, both atoms are in the transverse ground state. For the closed channel, atoms are in the transverse excited states
- The energy difference between the open and the closed channels is given by the transverse confinement energy and can be tuned by the external confinement potential.
- The single-particle eigenstate has cylindrical symmetry, but the short-range potential has spherical symmetry. The incompatibility of two symmetries naturally leads to coupling between channels.

With this understanding, resonance occurs when a bound state in the closed channel matches the scattering threshold of an open channel. Here, the energy offset between the closed channel and the open channel is typically $\hbar\omega = 2\hbar^2/(ma_\perp^2)$, and the bound state energy in three dimensions is estimated by $-\hbar^2/(ma_{\text{s}}^2)$. Thus, the resonance condition can be roughly estimated as

$$\hbar\omega - \frac{\hbar^2}{ma_{\text{s}}^2} = 0, \tag{2.84}$$

which leads to

$$\frac{a_\perp}{a_{\text{s}}} = \sqrt{2}. \tag{2.85}$$

https://doi.org/10.1017/9781108595216.003 Published online by Cambridge University Press

This is not that different from the exact results in Eq. 2.83 where $\sqrt{2}$ is replaced by 1.46 .... A similar argument can be applied to confinement into quasi two dimensions, or mixed dimensions. Here mixed dimensions means that one atom is confined to the d_1 dimension and the other atom is confined to the d_2 dimension, where both d_1 and d_2 can take a value between 0 and 3.[5]

2.6 Efimov Effect

In the above sections, we discussed different methods, as well as a general framework, to tune the two-body interaction potential to a scattering resonance. A quantum many-body system with such a resonant interaction potential has many intriguing properties, as we will discuss in Chapter 5 and Chapter 6. Here, before studying many-body physics, we first study a manifestation of resonant interaction in a three-body system. This problem can be generally solved by a so-called hyper-spherical coordinate approach [21, 22], but the calculation is quite involved. Here, to illustrate the essential physics, we take a simpler case of one light atom interacting with two heavy atoms, and we can utilize the Born–Oppenheimer approximation to simplify the calculation [141].

Born–Oppenheimer Approximation. First of all, we fix the positions of two heavy atoms with mass M at $\mathbf{R}/2$ and $-\mathbf{R}/2$, respectively, and study the motion of the light atom with mass m in the presence of these two heavy atoms. The Hamiltonian for the light atom therefore reads

$$\hat{H} = -\frac{\hbar^2\nabla^2}{2m} + \frac{2\pi\hbar^2 a_s}{m}\delta(\mathbf{R}_+)\frac{\partial}{\partial|\mathbf{R}_+|}|\mathbf{R}_+| + \frac{2\pi\hbar^2 a_s}{m}\delta(\mathbf{R}_-)\frac{\partial}{\partial|\mathbf{R}_-|}|\mathbf{R}_-|, \tag{2.86}$$

where $\mathbf{R}_\pm = \mathbf{r} \pm \mathbf{R}/2$, and we take $m \ll M$ such that the reduced mass is simplified as m. In the regime $\mathbf{r} \neq \pm\mathbf{R}/2$, let us consider the following three requirements: (i) the wave function should be an eigenstate of the kinetic operator; (ii) we consider that the light atom forms a bound state around both the two heavy atoms; and (iii) the wave function is symmetric or antisymmetric with respect to exchanging $\mathbf{R}_+$ and $\mathbf{R}_-$. Thus, we can write down the wave function as

$$\Psi_\pm(\mathbf{r}) \propto \frac{\exp\{-\kappa|\mathbf{R}_+|\}}{|\mathbf{R}_+|} \pm \frac{\exp\{-\kappa|\mathbf{R}_-|\}}{|\mathbf{R}_-|}, \tag{2.87}$$

where κ is real and positive. The energy of this wave function is $-\hbar^2\kappa^2/(2m)$.

Expanding the wave function around either $|\mathbf{R}_+|$ or $|\mathbf{R}_-|$ yields

$$\Psi_\pm \propto \frac{1}{|\mathbf{R}_\pm|} - \kappa \pm \frac{e^{-\kappa R}}{R} + \ldots, \tag{2.88}$$

[5] The exceptions are that they cannot both be 0 where no scattering state can be defined, and they cannot both be 3 when no confinement is applied at all.

https://doi.org/10.1017/9781108595216.003 Published online by Cambridge University Press

where $R = |\mathbf{R}|$, and the pseudo-potential requires the short-range behavior of the wave function to be

$$\Psi_{\pm} \propto \frac{1}{|\mathbf{R}_{\pm}|} - \frac{1}{a_s}. \tag{2.89}$$

Thus, it leads to

$$\kappa \mp \frac{e^{-\kappa R}}{R} = \frac{1}{a_s}. \tag{2.90}$$

Clearly, the term with a plus sign in the l.h.s. of Eq. 2.90 has no solution for negative and infinite a_s. So we consider the equation with a minus sign, resulting from the symmetric wave function in Eq. 2.87. The solution in general has the form

$$\kappa = \frac{1}{R} f\left(\frac{R}{a_s}\right), \tag{2.91}$$

where $f(y)$ is the solution to the equation $x - e^{-x} = y$. One can see that at unitarity with $a_s = \infty$ and $y = 0, f(0)$ is a constant. Therefore, $\kappa \sim 1/R$, and the energy is proportional to $-\hbar^2/(mR^2)$.

Continuous and Discrete Scaling Symmetry. With the help of the Born–Oppenheimer approximation, we have found that, at two-body resonance, the light atom induces an effective potential $\sim -\hbar^2/(mR^2)$ between two heavy atoms. Then, the Schrödinger equation for two heavy atoms is given by

$$\left(-\frac{\hbar^2 \nabla_{\mathbf{R}}^2}{M} - \frac{\hbar^2 c_0^2}{mR^2}\right) \Psi = E\Psi, \tag{2.92}$$

where c_0^2 is a constant. The most important feature of this equation is that the interaction energy scales the same way as the kinetic energy under a scaling transformation $\mathbf{R} \to \lambda \mathbf{R}$. Therefore, it looks as though, by applying this scale transformation, if E is an eigenenergy, E/λ^2 is also an eigenenergy. This works for any λ, which is known as the *continuous scaling symmetry*. However, if this is true, that also implies that the energy spectrum of this Hamiltonian is not bound from below. Hence, we need to apply an extra short-range cutoff to bound the spectrum from below. This short-range boundary condition can be a nonuniversal one depending on short-range details. And the fact that an extra nonuniversal high-energy cutoff is required also means that a theory with zero-range interaction potential is not renormalizable in this case.

Here we explicitly show how the extra short-range boundary condition affects the scaling symmetry. Since here we are interested in a three-body bound state, and since above we have considered that the light atom already forms a bound state with both heavy atoms, we now need only consider the bound state solution between these two heavy atoms. In the spherical coordinate of $\mathbf{R}$, we write $\Psi(\mathbf{R}) = \chi(R)/R$, as we now only consider the s-wave solution when two heavy atoms are bosons or distinguish particles. The Schrödinger equation for $\chi(R)$ is written as

$$\left[-\frac{\hbar^2}{M}\frac{d^2}{dR^2} - \frac{\hbar^2 c_0^2}{mR^2}\right] \chi = E\chi. \tag{2.93}$$

https://doi.org/10.1017/9781108595216.003 Published online by Cambridge University Press

Now we consider a zero-energy solution, or alternatively speaking, we consider the wave function at a distance when $E \ll 1/R^2$. Because of the scaling symmetry, we can assume $\chi = R^s$, and by setting $E = 0$, Eq. 2.93 gives

$$s(s-1) + \frac{c_0^2 M}{m} = 0. \tag{2.94}$$

This leads to $s = 1/2 \pm is_0$, where $s_0 = \sqrt{\frac{c_0^2 M}{m} - \frac{1}{4}}$, and we consider $M \gg m$ such that s_0 is always real. Thus, the two independent solutions can be written as

$$\chi_\pm = \sqrt{R} R^{\pm i s_0} = \sqrt{R} e^{\pm i s_0 \ln R}. \tag{2.95}$$

Each of $\chi_\pm$ is still invariant under a continuous scaling transformation, but because of the short-range boundary condition, the general wave function should be a superposition of both χ_+ and χ_- to satisfy the boundary condition. Note that the two solutions can also be written as $\sqrt{R}\cos(s_0 \ln R)$ and $\sqrt{R}\sin(s_0 \ln R)$, and so a general solution can be constructed as

$$\chi(R) = \sqrt{R}\cos(s_0 \ln R + \theta), \tag{2.96}$$

where θ should be determined by the short-range boundary condition. Clearly the wave function Eq. 2.96 is no longer invariant under a continuous scaling transformation, but if the scaling factor $\lambda = e^{\pi n/s_0}$, where n is an integer, the wave function is still invariant. This is known as the *discrete scaling symmetry*, because the scaling factor can only take values in a set of discrete numbers. Under the discrete scaling transformation, the energy becomes $E \to Ee^{-2\pi/s_0}$. That is to say, if E_0 denotes the lowest-energy bound state, and E_n denotes the nth bound state counting from below, then there is an infinite number of bound states, and their binding energies satisfy

$$E_n = E_{n-1} e^{-2\pi/s_0}. \tag{2.97}$$

Note that the solutions are actually the binding energies of the three-atom bound state, which means that the three-body bound state energies obey a geometric sequence. This result was first obtained by Efimov from solving the problem of three identical bosons nearby a two-body resonance and thus is named the *Efimov effect*. The Efimov effect in a three-body system was first experimentally found in cold ^{133}Cs gas of identical bosons [94], and later was also found between two bosons and a third distinguishable atom, or three distinguishable atoms [21, 22]. The discrete scaling symmetry has also been confirmed experimentally [176, 143].

Here we highlight that, from the symmetry perspective, the defining property of the Efimov effect is the discrete scaling symmetry with a universal scaling factor, which resulted from a Hamiltonian with continuous scaling symmetry plus a nonuniversal short-range boundary condition. We emphasize that this defining property has at least two nontrivial points:

- In many cases, a short-range boundary condition completely breaks the continuous scaling symmetry, but in this case, it still leaves a discrete scaling symmetry. Mathematically, it happens when Eq. 2.94 for s has a pair of conjugate solutions.

https://doi.org/10.1017/9781108595216.003 Published online by Cambridge University Press

- Although the short-range boundary condition is nonuniversal, the scaling factor is actually universal. In this case, one can see that although θ is a nonuniversal value depending on the details of the short-range boundary condition, and the exact value of the lowest binding energy E_0 is also nonuniversal, the scaling factor e^{π/s_0} is a constant only depending on the mass ratio and does not depend on the short-range details.

This definition of the Efimov effect from the symmetry perspective allows one to generalize this effect beyond few-body physics and to find more intriguing manifestations of this effect in many-body systems. One such example is the quantum many-body expansion dynamics of a scaling-invariant quantum gas in a specially designed expanding harmonic trap, which follows the same symmetry definition and is named the *Efimovian expansion* [48].

Finally, let us briefly discuss how these three-body bound states behave when the interaction is tuned away from the resonance. It turns out that when a_s is negative, the effective attraction is weaker than $\sim -1/R^2$ at large distance, which first affects these shallow bound states whose wave functions are more extended and have more weight on the long-range part. The energies of these bound states will increase as the interaction is tuned away from the resonance to the negative side, and they will in turn merge into the three-body continuum, as shown in Figure 2.7. When one of the three-body bound states meets the three-body threshold, it yields a three-body scattering resonance. When a_s is positive, the effective attraction is deeper than $\sim -1/R^2$. However, on this side, there also exists a two-body bound state, and as we have discussed in Section 2.1, the dimer energy is $-\hbar^2/(ma_s^2)$. Hence, the atom-dimer threshold energy is $-\hbar^2/(ma_s^2)$. It turns out that the increasing of the three-body binding energy is slower than the increasing of the two-body binding energy

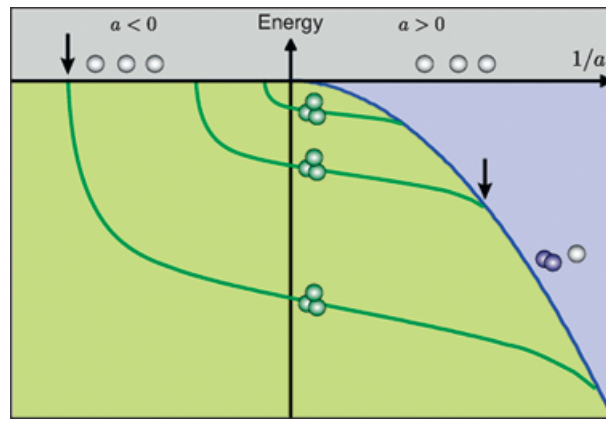

Figure 2.7 Three-body Efimov effect. The energy of three-body bound state of spinless bosons as a function of two-body scattering length a_s (a in the figure). The three-atom threshold is always $E = 0$. The atom-dimer threshold behaves as $-\hbar^2/(ma_s^2)$ in the positive a_s side. Three typical spectrum lines for the three-body bound state energy are shown. At resonance when $1/a_s = 0$, the binding energies form a geometric sequence. Two arrows label examples of three-atom scattering resonance and atom-dimer scattering resonance, respectively. Reprinted from Ref. [55]. A color version of this figure can be found in the resources tab for this book at cambridge.org/zhai.

https://doi.org/10.1017/9781108595216.003 Published online by Cambridge University Press

as $1/a_s$ increases; therefore, the three-body bound state will in turn merge into the atom-dimer continuum when the interaction is tuned away from the resonance to the positive side, as also shown in Figure 2.7. When one of the three-body bound states meets the atom-dimer threshold, it yields an atom-dimer scattering resonance. Both the three-atom resonance and the atom-dimer resonance will manifest in the loss rate of atoms, which can be experimentally measured as evidence of the Efimov effect [94, 176, 143].

2.7 From Few to Many

In this chapter, we have discussed two- and three-body problems. In the next chapter, we will start to discuss many-body physics in ultracold atomic gases. Here we would like to point out that there are many connections between few- and many-body problems in ultracold atomic physics. First of all, few-body problems help us to build up the right model for many-body physics, as we have discussed in Section 2.2 and Section 2.4. Second, few-body problems help us to locate the parameter regimes where the many-body physics can be interesting. We discussed in Section 2.4 and Section 2.5 how to tune the elastic scattering to be very strong. In addition, there is another important aspect that we do not discuss in this book, which is about the inelastic part of the scattering process. The inelastic part of the scattering process leads to atom loss. A strong inelastic scattering can lead to strong loss and, therefore, a short lifetime of the many-body system. Hence, in order that intriguing many-body physics takes place, we not only require the elastic scattering to be strong enough but also require the inelastic scattering not to be too strong. We need the solutions of the few-body problem to help us locate such regimes.

Third, few-body problems provide an alternative way to analyze correlations in a quantum many-body system. Generally speaking, there are two different approaches to studying many-body corrections, which are known as the top-down approach and the bottom-up approach. Here the top-down means starting from large-scale, long-wave length, or low-energy structures. Various kinds of mean-field theories that we will discuss in the next chapter belong to the top-down approach. In contrast, the bottom-up approach means understanding correlations in a many-body system from its microscopic building blocks, that is to say, from two-body, three-body, and then gradually adding more particles. The advances in ultracold atomic experiments allow us to control atom number very precisely, which makes this approach even experimentally possible. In experiments, one can observe how the many-body correlation gradually builds up by adding to the atom number one by one [197]. Theoretically, one systematic method to carry out this bottom-up approach is in fact the high-temperature expansion. This expansion uses the fugacity as a small parameter, and therefore it also works in the resonance when the interaction is very strong. Below we will briefly discuss this approach.

We consider the partition function $\mathcal{Z}$ at high temperature. At high temperature, μ is very negative and the fugacity $z = e^{\mu/(k_B T)}$ is very small. Hence we can use z as a small parameter to expand $\mathcal{Z}$ as

https://doi.org/10.1017/9781108595216.003 Published online by Cambridge University Press

$$\mathcal{Z} = \mathrm{Tr} e^{-(H-\mu N)/(k_B T)} = 1 + z \sum_{n_1} e^{-E_{n_1}/(k_B T)} + z^2 \sum_{n_2} e^{-E_{n_2}/(k_B T)} + \ldots, \tag{2.98}$$

where we have taken the $N = 1$ in the second term of Eq. 2.98 and n_1 denotes quantum numbers of all single-particle eigenstates, and $N = 2$ for the third term in Eq. 2.98 and n_2 denotes the quantum numbers of all two-particle eigenstates. For a uniform system,

$$\sum_{n_1} e^{-E_{n_1}/(k_B T)} = \sum_{\mathbf{k}} e^{-\hbar^2 \mathbf{k}^2/(2mk_B T)} = V \left(\frac{mk_B T}{2\pi\hbar^2}\right)^{3/2} = \frac{V}{\lambda^3}, \tag{2.99}$$

where $\lambda = \sqrt{2\pi\hbar^2/(mk_B T)}$ is the thermal de Broglie wavelength. E_{n_2} contains the center-of-mass motion $\mathbf{K}^2/(4m)$ and the relative motion with eigenenergies denoted by ϵ_{rel}. Since the center-of-mass and relative coordinates are separable, we have

$$\sum_{n_2} e^{-E_{n_2}/(k_B T)} = V \left(\frac{\sqrt{2}}{\lambda}\right)^3 \sum_{\epsilon_{\mathrm{rel}}} e^{-\epsilon_{\mathrm{rel}}/(k_B T)}. \tag{2.100}$$

Thus, the solution of the two-body problem allows us to obtain the partition function to the order of z^2. Furthermore, with the solutions of the three-body problem, we can obtain information on the partition function up to z^3, and this expansion can be systematically carried on. Here, for simplicity, we only consider the z^2 order.

Up to the z^2 order, we can therefore rewrite the partition function as

$$\mathcal{Z} = \mathcal{Z}^0 + V z^2 \left(\frac{\sqrt{2}}{\lambda}\right)^3 b_2, \tag{2.101}$$

where $\mathcal{Z}^0$ is the partition function in the absence of interactions, and

$$b_2 = \sum_{\epsilon_{\mathrm{rel}}} \left(e^{-\epsilon_{\mathrm{rel}}/(k_B T)} - e^{-\epsilon^0_{\mathrm{rel}}/(k_B T)} \right). \tag{2.102}$$

Here b_2 is called the second *virial coefficient*, and $\epsilon^0_{\mathrm{rel}}$ is the eigenstate for relative motion in the absence of interactions. Below we shall discuss how to compute b_2 with the knowledge of two-body problem discussed in Section 2.1 [86].

For the reason we discussed in Section 2.1, we ignore the interaction effect in all high partial wave channels and only consider the interaction effect in the *s*-wave channel. Note that b_2 can be rewritten as

$$b_2 = \sum_{n_b} e^{-E_{n_b}/(k_B T)} + \int_0^{+\infty} dk (g(k) - g_0(k)) e^{-\hbar^2 k^2/(mk_B T)}, \tag{2.103}$$

where the first contribution comes from bound states due to interactions and E_{n_b} denotes binding energies, and the second contribution comes from all scattering states in the *s*-wave channel; $g(k)dk$ and $g_0(k)dk$ denote the number of eigenstates with wave vector between k and $k + dk$ for interacting systems and noninteracting systems, respectively. As we have shown in Section 2.1, the wave function for the relative motion between two particles in the *s*-wave channel can be written as

$$\Psi = \frac{\sin(kr + \delta_k)}{r}. \tag{2.104}$$

https://doi.org/10.1017/9781108595216.003 Published online by Cambridge University Press

Considering a spherical box with radius size R, the wave function has to satisfy the boundary condition at $r = R$, which yields

$$kR + \delta_k = s\pi, \tag{2.105}$$

where s is an integer. Eq. 2.105 gives

$$\left(R + \frac{d\delta_k}{dk}\right)\Delta k = \pi \Delta s. \tag{2.106}$$

The number of eigenstates increases by 1 when Δs increases by 1, which requires Δk increasing by

$$\Delta k = \frac{\pi}{R + \frac{d\delta_k}{dk}}. \tag{2.107}$$

Thus, we have

$$g(k)dk = \frac{1}{\pi}\left(R + \frac{d\delta_k}{dk}\right)dk, \tag{2.108}$$

and for the noninteracting case, $g_0(k)dk = Rdk/\pi$. Therefore, b_2 can be written as

$$b_2 = \sum_{n_b} e^{-E_{n_b}/(k_B T)} + \frac{1}{\pi}\int_0^\infty \frac{d\delta_k}{dk} e^{-\hbar^2 k^2/(mk_B T)} dk. \tag{2.109}$$

Using $\tan\delta_k = -ka_s$, one can obtain

$$\begin{aligned}\int_0^\infty \frac{d\delta_k}{dk} e^{-\hbar^2 k^2/(mk_B T)} dk &= -\mathrm{sgn}(a_s)\int_0^\infty \frac{|a_s|}{(k|a_s|)^2 + 1} e^{-\hbar^2 k^2/(mk_B T)} dk \\ &= -\mathrm{sgn}(a_s)\frac{\pi}{2}\mathrm{Erfc}[\alpha]e^{\alpha^2},\end{aligned} \tag{2.110}$$

where sgn is the sign function, Erfc is the complementary error function, and $\alpha = \lambda/(\sqrt{2\pi}|a_s|)$. Hence, if one excludes the contribution from the bound state,

$$b_2 = -\mathrm{sgn}(a_s)\frac{1}{2}\mathrm{Erfc}[\alpha]e^{\alpha^2}. \tag{2.111}$$

As shown in Figure 2.8(a), b_2 decreases from zero to $-1/2$ if a_s increases from zero to positive infinite and increases from zero to $1/2$ if a_s decreases from zero to negative infinite. This jump of unity at resonance can be exactly compensated by a zero-energy bound state contribution. Including the contribution from the bound state, b_2 becomes a smooth function when a_s changes from negative infinite to positive infinite, and b_2 monotonically increases as $-\lambda/a_s$ decreases.

With the help of the partition function, one can show that the total energy can be deduced as [72]

$$\mathcal{E} = \frac{3nk_B T}{2}\left(1 + \frac{n\lambda^3}{2^{7/2}}\right) + \mathcal{E}_{\mathrm{int}} = \mathcal{E}_{\mathrm{kin}} + \mathcal{E}_{\mathrm{int}} \tag{2.112}$$

and

$$\mathcal{E}_{\mathrm{int}} = \frac{3nk_B T}{2}(n\lambda^3)\left[-\frac{b_2}{\sqrt{2}} + \frac{\sqrt{2}}{3}T\frac{\partial b_2}{\partial T}\right], \tag{2.113}$$

https://doi.org/10.1017/9781108595216.003 Published online by Cambridge University Press

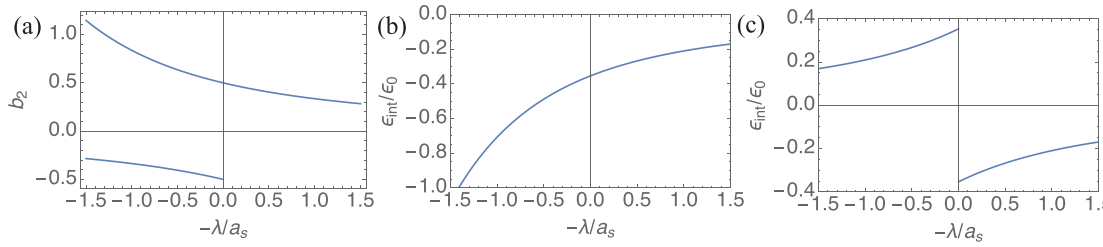

Figure 2.8 High-temperature expansion. (a) The second virial coefficient b_2 as a function of $-\lambda/a_s$. For positive a_s, the positive b_2 branch includes the contribution from the shallow bound state and smoothly connects to the negative a_s side, and the negative b_2 branch excludes the contribution from the shallow bound state. (b–c) The interaction energy $\mathcal{E}_{\rm int}$ in units of $\mathcal{E}_0 = 3nk_{\rm B}T(n\lambda^3)/2$ as a function of $-\lambda/a_s$ (b) with and (c) without the bound state contribution.

where n is the density of the system. With b_2, one can straightforwardly obtain the interaction energy with or without the contribution from the bound state, as shown in Figures 2.8(b) and (c), respectively. One can see that, including the bound state contribution, the interaction energy is always negative, consistent with the fact that the underlying potential is attractive. For positive scattering length, when the bound state contribution is excluded, the interaction energy is positive, which is called the *upper branch*. When the bound state contribution is included, the interaction energy is negative, which is called the *lower branch*. We will come back to revisit this physics in the discussion of polarons in Section 5.2. When the bound state contribution is excluded, one can see that the interaction energy becomes small when $a_{\rm s}$ is small, consistent with our discussion in Section 2.1 that the amplitude of $a_{\rm s}$ characterizes interaction strength when $|a_{\rm s}|$ is small. One can also see that the interaction energy remains finite even when $a_{\rm s}$ is infinite at resonance, and the interaction energy becomes proportional to the thermal kinetic energy at resonance. That the interaction energy scales the kinetic energy characterizes strong interaction effects, as we will discuss again in Chapter 6.

Exercises

2.1 Calculate the scattering length for a three-dimensional square well interaction potential $V(r) = 0$ for $r > r_0$, $V(r) = -V_0$ for $r_0 > r > 0$ with $V_0 > 0$, and $V(r) = \infty$ for $r = 0$. Discuss how the scattering length changes as a function of V_0, and discuss when the binding energy satisfies the relation $E = -\hbar^2/(2\bar{m}a_{\rm s}^2)$.

2.2 Calculate the scattering length for a three-dimensional hard core potential $V(r) = 0$ for $r > r_0$, $V(r) = V_0$ for $r_0 > r > 0$ with $V_0 > 0$, and $V(r) = \infty$ for $r = 0$. Discuss how the scattering length changes as a function of V_0 and the difference from the square well potential above.

2.3 Show that for a finite range interaction $V(r) \simeq 0$ for $r > r_0$, the phase shift for the lth partial wave $\delta_l \propto k^{2l+1}$.

https://doi.org/10.1017/9781108595216.003 Published online by Cambridge University Press

2.4 Show that the bound state wave function $\Psi = \chi/r$ with χ given by Eq. 2.12 also satisfies the Schrödinger equation 2.18 with $V(r)$ given by $\delta(r)\hat{O}(r)$ and $\hat{O}(r)$ given by Eq. 2.21.

2.5 Analytically show that

$$\frac{1}{V}\sum_{\mathbf{p}}\left(\frac{1}{E-\hbar^2\mathbf{p}^2/m+i0^+}+\frac{1}{\hbar^2\mathbf{p}^2/m}\right)=-\frac{ikm}{4\pi\hbar^2}, \tag{2.114}$$

where $k=\sqrt{mE/\hbar^2}$.

2.6 Derive the general interaction form between two spin-2 atoms.

2.7 Show Eq. 2.62 for a finite energy scattering state using the simplified two-channel model discussed in this chapter.

2.8 (1) Show that the two-body T-matrix for the two-channel model is given by Eq. 2.66, following the same method of summing up the ladder diagram shown in Figure 2.3(b). (2) Verify the normalization conditions of Eq. 2.67–2.69 by comparing the two-body T-matrix (Eq. 2.66) with $T_2(E=0)=4\pi\hbar^2 a_s/m$ and a_s given by Eq. 2.61.

2.9 Use a variational wave function to show that the lowest eigenenergy of the Hamiltonian Eq. 2.92 is not bound from below if no short-range cutoff is imposed.

2.10 With the help of Eq. 2.90, discuss the effective three-body interaction potential when a_s is away from infinite.

2.11 Compute the chemical potential and the pressure up to z^2 order by using the high-temperature expansion.

https://doi.org/10.1017/9781108595216.003 Published online by Cambridge University Press